Nitroxide-derived pyrimidines for noncovalent spin-labeling of nucleic acids

Gunnar Birgir Sandholt

Faculty of Physical Sciences
University of Iceland
2012

Nitroxide-derived pyrimidines for noncovalent spin-labeling of nucleic acid

Gunnar Birgir Sandholt

90 ECTS thesis submitted in partial fulfillment of a
Magister Scientiarum degree in chemistry

Advisor
Snorri Þór Sigurðsson

Faculty Representative
Guðmundur G. Haraldsson

Faculty of Physical Sciences
School of Engineering and Natural Sciences
University of Iceland
Reykjavik, October 2012

Nitroxide-derived pyrimidines for noncovalent spin-labeling of nucleic acids
Modified pyrimidines for noncovalent spin-labeling
90 ECTS thesis submitted in partial fulfillment of a Magister Scientiarum degree in chemistry

Faculty of Physical Sciences
School of Engineering and Natural Sciences
University of Iceland
VRII, Hjarðarhagi 2-6
107, Reykjavik
Iceland

Telephone: 525 4000

Bibliographic information:
Gunnar Birgir Sandholt, 2012, Nitroxide-derived pyrimidines for noncovalent spin-labeling of nucleic acids, Master's thesis, Faculty of Physical sciences, University of Iceland, pp. 52.

ISBN XX

Printing: Háskólaprent ehf.
Reykjavik, Iceland, October 2012

Abstract

To understand the function of nucleic acids in biological systems, their structural information is important. Electron paramagnetic resonance (EPR) spectroscopy has been increasingly used to study spin-labeled nucleic acids. Spin labels are usually incorporated site-specifically through covalent bonding, which can be difficult and time consuming. A new method was previously developed in our lab using noncovalent interactions where a spin label binds to an abasic site in a duplex DNA at low temperatures. However, the spin label (**ç**) that was used has a lengthy synthetic route and limited solubility in aqueous solutions. To search for spin labels with higher affinity for abasic sites and easier synthesis we have incorporated several nitroxides into the 5-position of pyrimidines. Two were made by an azide-alkyne Huisgen-Meldal-Sharpless (3+2) cycloaddition reaction (click reaction) and another two using palladium-catalyzed Sonogashira coupling. Among the click spin-labels, a U-analogue was fully bound at -30 °C while ca. 60% of a C-analogue bound to a duplex DNA containing an abasic site when placed opposite to A and G, respectively. However, 5-alkyne-linked pyrimidine spin-labeled derivatives of U and C bind only ca. 30% and 90% when paired with A and G, respectively. A C-analogue prepared by coupling 4-amino-TEMPO to 4-TPS U-derivative did not bind at all. Combined, our results indicate that stacking interactions contribute significantly to noncovalent binding of spin-labels at abasic sites in duplex DNA. Further work involving conjugation of a polyamine linker and an intercalator to the 1-position of the pyrimidines was initiated.

Ágrip

Upplýsingar um byggingu kjarnsýra eru mikilvægar til að skilja hvernig þær virka í líffræðilegum kerfum. Rafeindaspunatækni (Electron paramagnetic resonance) hefur undanfarið verið notuð í rannsóknum á spunamerktum kjarnsýrum. Spunamerkin eru oftast innleidd staðbundið með samgildum tengjum, sem getur verið tímafrekt. Ný aðferð hefur nýlega verið þróuð, á rannóknastofunni okkar, þar sem merkin eru innleidd staðbundið án samgildra tengja á óbasaða stöðu í DNA tvíliðu, gegnum vetnistengi og π-stöflun við lágan hita. Merkið sem um ræðir (**ç**) hefur langan efnasmíðaferil og takmarkaða leysni í vatnslausnum. Við leit að merkjum sem útbúa má með auðveldari efnasmíði og bindast betur við óbasaða stöðu, höfum við smíðað nokkrar afleiður pyrimidína sem innihalda nítroxíð. Tvö merki voru smíðuð með azíð-alkýn Huisgen-Medal-Sharpless (3+2) hringálagningu (smelliefnafræði) og önnur tvö með því að nota palladium-hvataða Sonogashira-kúplun nítroxíðs við stöðu 5 á pýrímidín bösunum. Á meðal smellispunamerkjanna bast U afleiðan að fullu í óbasaða stöðu á móti A í tvíhliða DNA við -30 °C, á meðan C afleiðan bast 60% við G. Aftur á móti bundust alkyn tengdu spunamerkin ekki eins vel, U afleiðan tengdist aðeins 30% á móti A og C afleiðan 90% á móti G. C afleiða, sem var smíðuð með kúplun 4-amín-TEMPO við stöðu fjögur, sýndi enga bindingu. Niðurstöðurnar benda til þess að π-stöflun milli kirnibasa hafi meira vægi en vetnistengi á sækni basa í óbasaða stöðu í DNA tvíliðu. Hafist hefur verið handa við að tengja fjölamínkeðju með millibundnuefni á fyrsta stað á pýrimidinínu. Sú efnasmíð er í vinnslu.

Table of Contents

List of Figures

List of Schemes

List of Abbreviations

A	adenine
BER	base excision repair
C	cytosine
CW	continuous wave
DCE	dichloroethane
DMAP	dimethyl amino pyridine
DMF	*N,N*-dimethylformamide
DMSO	dimethylsulfoxide
DNA	deoxyribonucleic acid
EPR	electron paramagnetic resonance
FRET	fluorescence resonance energy transfer
G	guanine
HMDS	hexamethyldisilazane
K_d	dissociation constant
mRNA	messenger ribonucleic acid
m-CPBA	*meta*-chloroperbenzoic acid
µM	micromolar
NMR	nuclear magnetic resonance
NC-SDSL	noncovalent site-directed spin labeling
PELDOR	pulsed electron-electron double resonance
RNA	ribonucleic acid
rRNA	ribosomal ribonucleic acid
SDSL	site-directed spin labeling
T	thymine
TEMPO	2,2,6,6-tetramethylpiperidine-N-oxyl
TPS	triisopropyl sulphonyl
tRNA	transfer ribonucleic acid

Acknowledgement

I first of all want to thank my advisor Professor **Snorri Þór Sigurdsson** for his guidance and for pushing me to achieve my best throughout this project. Second of all I want to thank **Dr. Sandip A. Shelke** for his fountain of wisdom and for teaching me everything there is to know about working in a lab and giving me the edge to exceed in chemistry.

I also want to think my group members Kristmann Gíslason, Dnyaneshwar Gophane, Nitin Kunjir, Anil Jagtap, Supham Saha and Hörður Harðarson for their help and moral support during my time in the lab.

Finally, I want to thank my family for their support and everybody in Raunvísindastofnun Háskólans for being awesome.

1 Introduction

1.1 Nucleic acids

Nucleic acids store and transfer the genetic information from one generation to the next in all living organisms. Deoxyribonucleic acid (DNA) stores the information using a four letter code and ribonucleic acid (RNA) transfers that information into proteins. Although this is the most well known function of nucleic acids, in recent years there have been many discoveries of RNAs involvement in number of biological systems. RNA takes part in amino acid transfer, gene regulation, protein synthesis and has been discovered to be used as a catalyst and for ligand binding [1, 2].

All these versatile functions of nucleic acids are due to their unique structure and dynamics. Understanding the movement and conformational changes of biomolecules in biological systems is of great interest, not only to quench the curiosity about life in the universe and how it functions, but also for drug discovery, where the understanding of biological functions can lead to therapeutic methods that save lives.

Structural studies of nucleic acids have been done by several techniques. These techniques can be divided in two groups, high resolution techniques and low resolution techniques. The techniques complement each other in quality. High resolution techniques give very accurate information about the position and distance between atoms in three dimensional space. X-ray crystallography [3] and NMR spectroscopy [4] are good examples of high resonance techniques. X-ray crystallography is the most dominant method in giving precise structural conformation of large molecules. This method is very popular for structure determination of proteins while there are not many structures available for RNAs. The reason is that high-quality crystals of the molecule are needed, which is rarely possible for RNAs. Other disadvantage of X-ray crystallography is that molecules crystallize in the lowest energy configuration, which is not always the biologically active structure. There, a spectroscopic technique like NMR is preferred since NMR can be used to study biomolecules in their native form, although there have been difficulties in interpreting the data of molecules over 50 kDa, which makes this method size-limited. In addition, most nucleic acids require isotopic labeling, which is very expensive and time consuming.

Low resolution techniques can be used to monitor structural changes of molecules when interacting with other molecules [4, 5]. These techniques, like fluorescence resonance energy transfer (FRET) [6] and electron paramagnetic resonance (EPR) [7-10] use labels to study the structure. Structure determination of molecules with FRET and EPR relies on measuring distances and distance changes within a molecule between two labels in a molecule. Since the only things measured are the labels there are no size limitations. However, since labeling is necessary, big labels, when incorporated, can interfere with the function by distorting the shape of the nucleic acid and limited information is obtained about the part of the molecule which is not labeled.

1.2 EPR spectroscopy

Electron paramagnetic resonance (EPR) spectroscopy is used to study unpaired electrons. This method has become popular in recent years due to high specificity toward radicals and technical improvement. EPR is applicable for distance measurements within a molecule, were continuous wave (CW) EPR can measure distances of 8-25 Å [11] and pulsed EPR can measure distances up to 15-80 Å [8, 12, 13]. EPR is also very sensitive to the motion of paramagnetic centers, making it capable of detecting dynamics of the molecule. That information is crucial for the understanding function of nucleic acids in biological systems. Nucleic acids are diamagnetic and cannot be measured with EPR,

so radicals have to be incorporated into the molecules. Nitroxide radicals, like 4-oxo-2,2,6,6-tetramethyl-1-piperidinyloxy (4-oxo-TEMPO) [14] is favorable due to high stability under most conditions. Nitroxide spin-labels show three sharp lines in solution due to hyperfine coupling of the radical spin (S=1/2) to the nitrogen's (^{14}N) spin state (I=1) (**Figure 1**).

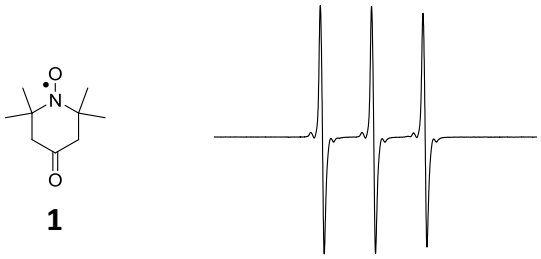

Figure 1. Structure of 4-oxo-TEMPO, a stable nitroxide radical (left) and its CW-EPR spectrum (right).

1.3 Spin labeling of nucleic acids

1.3.1 Techniques for spin-labeling nucleic acids

To be able to accurately study the structure and dynamics of nucleic acids by EPR spectroscopy, they need to be spin labeled at a predetermined site. This method is called site-directed spin labeling (SDSL) where spin labels can be attached to the base [15], sugar [16] and phosphate backbone [17] of the nucleic acid.

Today there are three SDSL methods for nucleic acids available. Two are covalently bound site-directed spin labeling approaches (**Figure 2A and B**) and the third, developed in our laboratory, is a noncovalent and site-directed spin labeling (NC-SDSL) strategy (**Figure 2C**), which will be discussed in detail in chapter 1.4.

The first two SDSL approaches incorporate labels by creating a covalent bond between the label and the nucleic acid. The First method is called post-synthetic labeling (**Figure 2A**) [9, 18, 19] were spin labels react to a specific reactive site in the nucleic acid. An advantage of this method is that many of the spin labels are commercially available and react easily, which can also be a disadvantage. Nucleic acids have many reactive sites, and having a label that reacts easily can cause unwanted side products that can be difficult to purify.

The second method is labeling during polymer synthesis (**Figure 2B**), where spin labels are incorporated during automatic synthesis of the nucleic acid, utilizing a spin-labeled phosphoramidite building block [9, 18, 19]. Here, incorporation of various spin labels is possible with high efficiency. This method requires time and specific skills along with the risk of partial reduction of the radical when it comes in contact with the chemicals used in the automatic synthetic process.

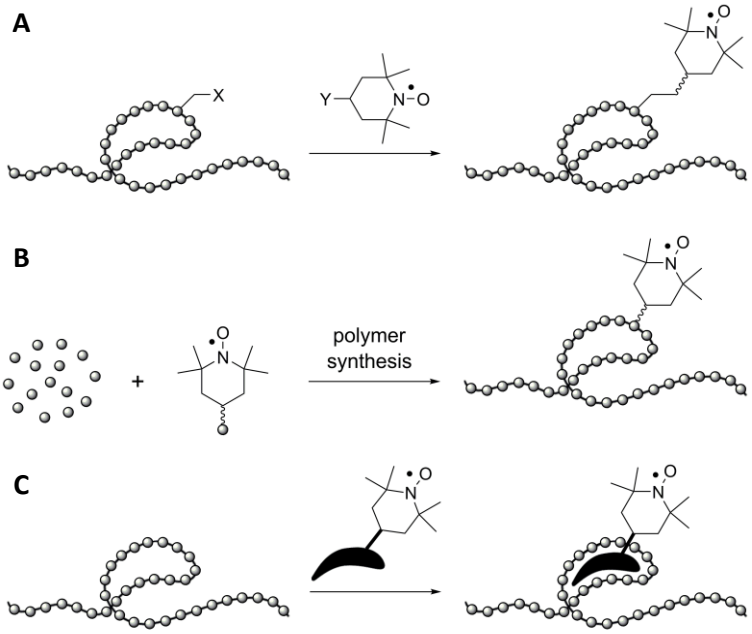

Figure 2. Cartoon representation of site-directed spin-labeling methods. **A**. Post-synthetic labeling **B**. Labeling during nucleic acid synthesis. **C**. Noncovalent labeling. TEMPO is shown as an example of nitroxide. Taken from [10].

To get around problems in the synthesis and purification steps, NC-SDSL was developed in our lab, which exploits noncovalent interactions of natural bases in nucleic acids [20] (**Figure 2C**). Here a base is removed, like occurs in Nature when damaged DNA is repaired enzymatically by cleavage of the glycosidic bond [21], leaving an abasic site to which the spin-labeled base **ç** can bind without covalent bonds, using only hydrogen bonding and π-stacking interactions (**Figure 3**). The abasic site is incorporated by using an abasic phosphoramidite building-block in the nucleic acid synthesis process.

1.4 Noncovalent and site-directed spin labeling with ç

The pyrimidine derivative, **ç**, used in the development of NC-SDSL is a cytosine fused with an oxazine linkage to a nitroxide-bearing isoindoline spin-label [20]. The cytosine derivative binds via three hydrogen bonds to the opposite guanine, between the flanking bases (**Figure 3**). The base opposite the abasic site is often called the orphan base because it lacks the base-pairing partner in a duplex DNA.

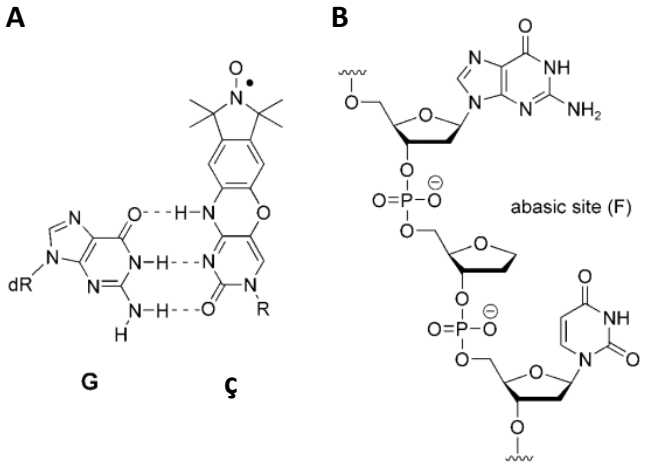

Figure 3. A. Base pairing of **ç** with orphan guanine (G) **B**. Abasic site in DNA [20].

The spectrum of **ç** in aqueous solution shows three narrow lines (**Figure 4B**). Slowing down the tumbling movement by lowering the temperature results in line broadening (**Figure 4C**). Therefore, when spin labels bind to nucleic acids, there is a large change in mobility. Large molecules, like nucleic acids, move slowly in solution, compared to the small freely rotating molecule like the **ç**, giving a broadened spectrum. Therefore, when **ç** is bound in the abasic site of the DNA, a slow-moving component appears both in the high- and low-field part of the spectrum at 0 °C (**Figure 4D**) and the fast-moving component reduces when the temperature is reduced until disappearing completely at -30 °C, indicating that **ç** is fully bound (**Figure 4E**).

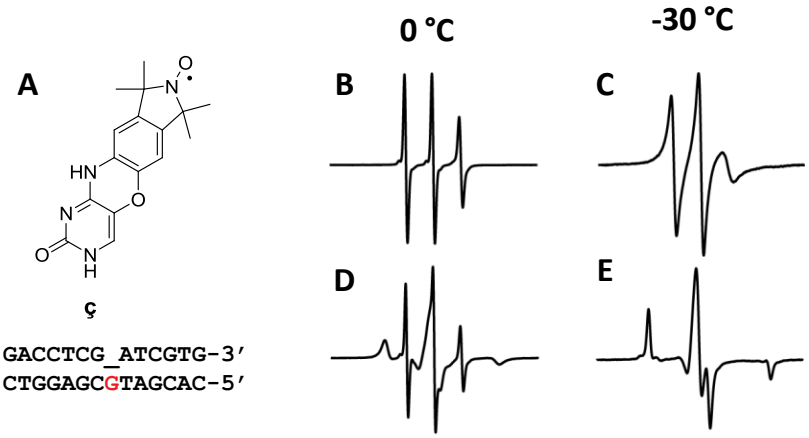

Figure 4. Binding studies of **ç** in an abasic site containing 14-mer duplex DNA. **A**. Structure of **ç** and the sequence of 14-mer abasic site containing duplex DNA. **B**. EPR spectrum of **ç** at 0 °C. **C**. EPR spectrum of **ç** at -30 °C. **D**. EPR spectrum of **ç** with 14-mer abasic site duplex DNA at 0 °C. **E**. EPR spectrum of **ç** with 14-mer abasic site duplex DNA at -30 °C [20].

1.4.1 Triazole-linked spin-labels for noncovalent and site-directed spin-labeling

Synthesis of **ç** requires substantial synthetic effort [20]; therefore spin labels with shorter and easier synthesis route that bind at higher temperature are preferred. Pyrimidine-modified nitroxides bearing an isoindoline connected to a base with a triazole linkage (**Figure 5**) were synthesized by Dr. Sandip A. Shelke and their binding affinity measured [22].

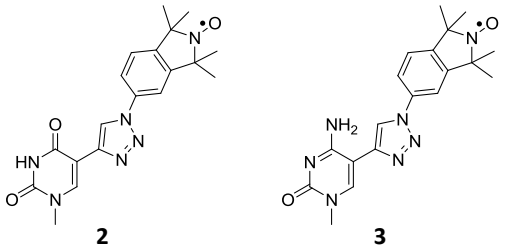

Figure 5. Structure of pyrimidine modified 5-triazole-linked spin-labels.

The synthetic routes of the triazole-linked spin labels are shorter than for **ç** (**Scheme 1 and 2**). The key step was a Huisgen-Meldal-Sharpless (3+2) cycloaddition reaction (click reaction) between the azide-modified isoindoline **7** [23] with alkynes **6** and **9** to give spin-labels **2** and **3**, respectively [22].

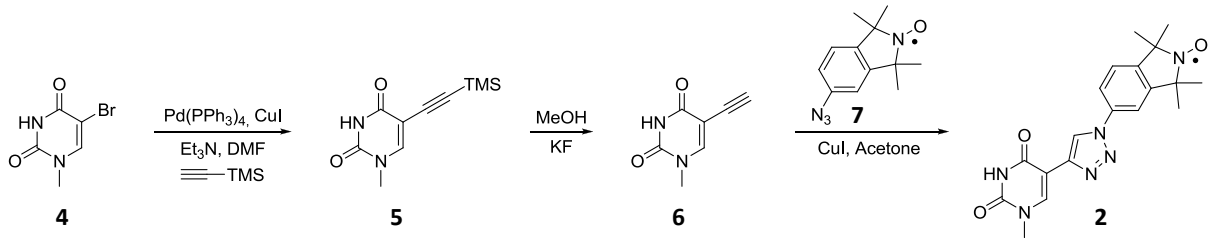

Scheme 1. Synthesis of an uracil-derived, triazole-linked spin-label for NC-SDSL.

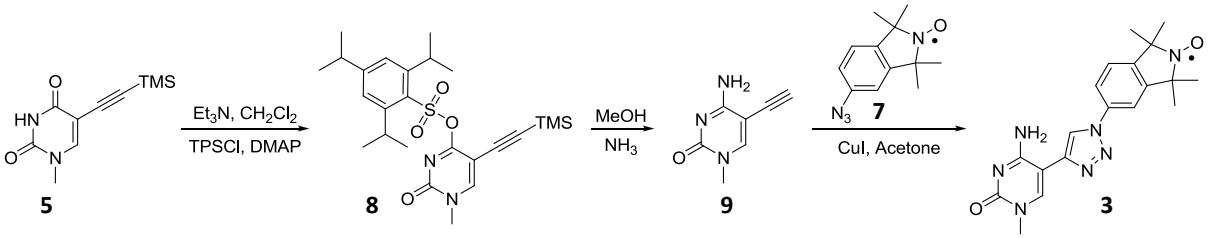

Scheme 2. Synthesis of a cytosine-derived, triazole-linked spin-label for NC-SDSL.

The uracil containing the triazole-linked spin label **2** bound fully to abasic site duplex DNA at -30 °C while the cytosine analogue bound ca. 60%. The low binding of the cytosine derivative was surprising since cytosine can in principle form one extra hydrogen bond compared to the uracil derivative.

Although triazole-linked spin labels have good binding and easier synthesis than **ç**, they lack rigidity. The triazole-linked spin-labels have two single bonds with free rotation that changes the position of the radical relative to the nucleic acid, giving a distance distribution when measured in pulsed EPR. This project sought to rectify that shortcoming.

1.5 Project goals

For the NC-SDSL approach to be feasible for structural studies of nucleic acids, readily available rigid spin-labels with high affinity and short and simple synthetic routes are desirable along with solubility in aqueous solutions.

The goal of the thesis project was to design and synthesize spin labels with high affinity towards abasic sites in duplex DNA that are conformationally unambiguous [24, 25] for accurate distance determination in nucleic acids. Having a molecule that is conformationally unambiguous means that rotation of single bonds in the linker does not cause a spatial displacement of the nitroxide relative to the molecule to which it is attached. The nitroxide radicals stay at the same position because the angle of the bond does not change, i.e. the N-O bond is on the the same axes as the rotation of the bonds as shown in our target molecules **10** and **11** (**Figures 6 and 7**).

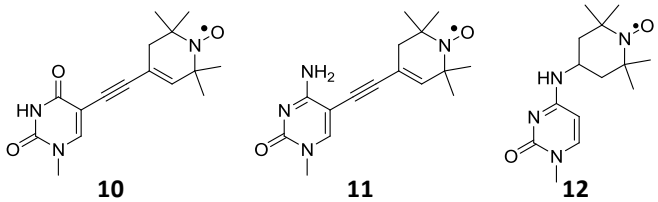

Figure 6. Structures of simple pyrimidine-modified spin labels. Uracil derived 5-alkyne-linked spin label **10** (left). Cytosine derived 5-alkyne-linked spin label **11** (middle). Cytosine derived 4-amino-TEMPO spin label **12** (right).

As mentioned before was our first criteria in our design to have spin labels that are conformationally unambiguous for accurate distance measurement. Accordingly, two spin labels were designed where

pyrimidines linked at 5-position via an alkyne link to a nitroxide bearing tetrahydropyridine moiety (**Figure 6**). Those labels fit the profile and have rotation around the single bonds next to the alkyne which does not affect the distance measurements. The third spin label was a cytosine analogue with 4-amino-TEMPO (**Figure 6**). When looking at the spin label **12** thoroughly, it is seen that due to chair formation of the pyridine moiety, the distance measurements will give minor distance curve when rotating the single bond linking the pyrimidine to the spin label. Spin labels **10** and **11** have a double bond in the pyridine moiety that flattens the label, despite that a small distance curve will be observed although being small. All labels had a methyl group at the N1-position because N1-methyl-derived **ç** had bound better than the unmodified version [26]. All these spin labels were expected to form hydrogen bonds to purines placed opposite the abasic site. The uracil label **10** will form two hydrogen bonds to adenine (A) and cytosine labels **11** and **12** will form three hydrogen bonds to guanine (G) (**Figure 7**).

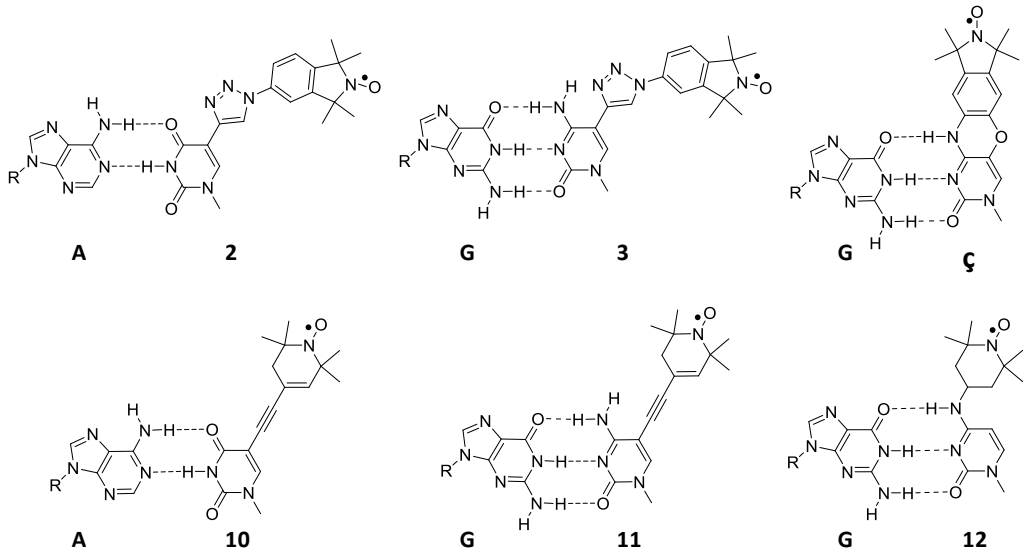

Figure 7. Base pairing of **ç** and the simple spin-labeled pyrimidines

Labels **10, 11** and **12** are not expected to stack as well as **ç** and the triazole-linked spin labels **2** and **3**, having limitied free π-electrons to stack with. The acetylene-linked spin labels provide an indirect measure of the importance of the triazole ring in stacking in abasic sites in duplex DNA.

If there are no simple spin labels with high affinity towards abasic site DNA, how can the affinity be increased? Lhomme et.al. attached adenine to a polyamine linker and a known intercalator to give excellent binding to abasic site DNA (K_a = 20 x 10^{-4} M^{-1}) [27]. The second part of the thesis was to implement Lhomme's strategy on existing pyrimidine-derived spin labels. The strategy is described in greater detail in section 2.5.

2 Results and discussion

In this chapter I will describe the syntheses and the EPR measurements. Synthesis of three simple spin-labels will be discussed in detail along with looking thoroughly at their EPR spectra in the presence of both DNA and RNA duplexes containing abasic sites. To conclude the chapter we will go through a synthetic route of spin label that has the potential to have higher affinity to an abasic site in duplex DNA.

2.1 Synthesis of 5-alkyne spin-labeled pyrimidines 10 and 11

The syntheses of 5-alkyne spin labeled pyrimidines **10** and **11** started with iodination of uracil, followed by regiolelective methylation via the corresponding trimethylsilyl derivative. Sonogashira coupling was performed on **15** using the acetylene spin-label **16** [28] in the presence of palladium and copper catalysts, which yielded spin label **10** (**Scheme 3**).

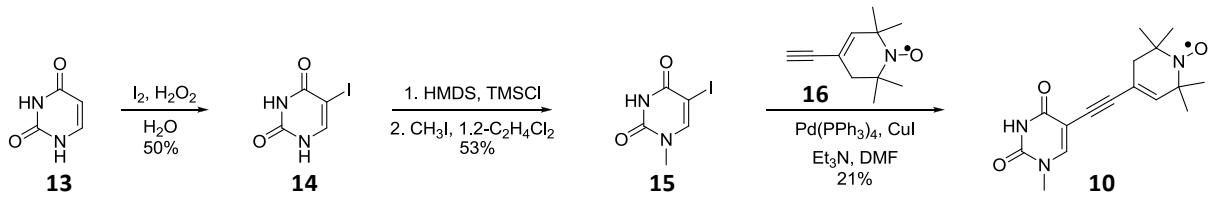

Scheme 3. Synthesis of uracil derived 5-alkyne-linked spin label **10** for NC-SDSL.

The cytosine derivative of the 5-alkyne-linked spin label was made from N1-methyl-5-iodo-uracil (**15**) by activating it to the 2,4,6-triisopropylbenzenesulfonyl (TPS) derivative before incubation with ammonia to give cytosine-derivative **18**. Sonogashira coupling was performed like before on the **18** using acetylene spin label **16** [28], yielding spin label **11** (**Scheme 4**).

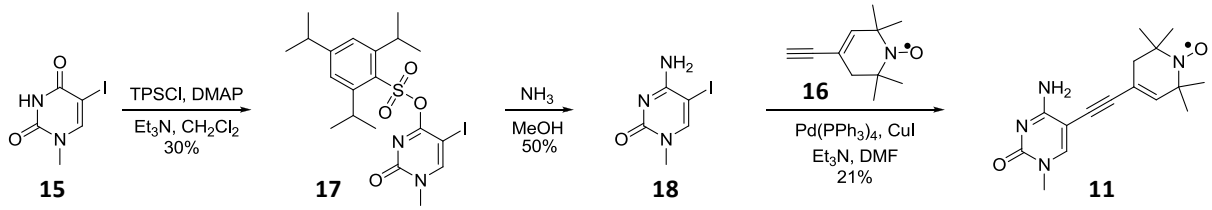

Scheme 4. Synthesis of cytosine derived 5-alkyne-linked spin label **11** for NC-SDSL.

2.2 Synthesis of 4-amino-TEMPO spin-labeled cytosine 12

Synthesis of the amino-linked spin-label **12** was performd using a similar method as used in preparation of **11**. Uracil was methylated regioselectively by first protecting the carboxyl group in situ using HMDS and TMSCl, followed by treatment with CH_3I which gave **19** in moderate yield. The 4-position was then activated by converting **19** to its OTPS derivative **20** prior to coupling the 4-amino-TEMPO, which afforded spin-label **12** (**Scheme 5**).

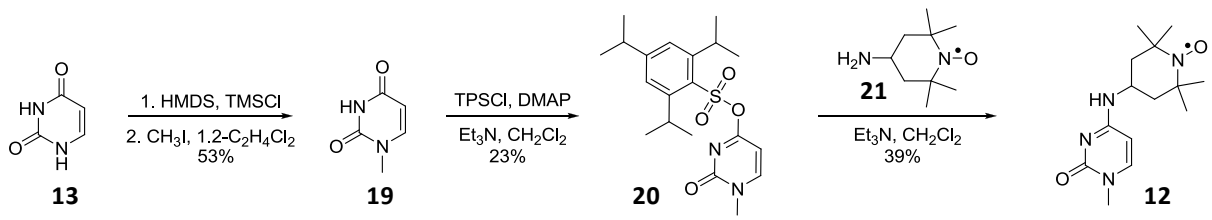

Scheme 5. Synthesis of cytosine derived 4-amino-linked spin label **12** for NC-SDSL.

2.3 Binding results for 4-amino and 5-alkyne labeled pyrimidines

Before we started to determine the biniding of the spin labels in an abasic site in duplex DNA we wanted to know how the spin-label spectra changed in correlation with the change in temperature. All samples were measured in a 30% ethylene glycol solution containing 2% DMSO, a solvent commonly used for PELDOR. DMSO is used to increase the solubility of spin labels in aqueous medium. Looking at the spectra we see that the signal broadens with reduced temperature (**Figure 8**).

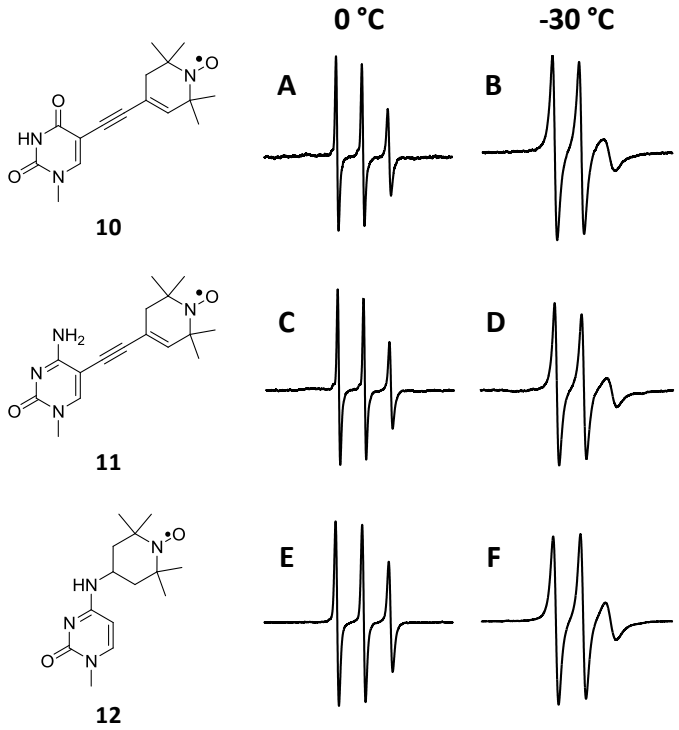

Figure 8. EPR measurements of spin-labels in aqueous solution at 0 and -30 °C. All measurements were conducted in phosphate buffer containing 30% aqueous ethylene glycol solution and 2% DMSO **A-B**. Spectra of uracil derived 5-alkyne-linked spin label **10** at 0 and -30 °C, respectively. **C-D**. Spectra of cytosine derived 5-alkyne-linked spin label **11** at 0 and -30 °C, respectively. **E-F**. Spectra of cytosine derived 4-amino-TEMPO spin label **12** at 0 and -30 °C, respectively.

2.3.1 Binding of spin-labels 10, 11 and 12 to DNA

The uracil derivative of the 5-alkyne-linked spin label **10** was measured in the presence of a 14-mer abasic site DNA with the adenine as the orphan base (**Figure 9**). EPR spectra showed no binding down to -10 °C (**Figure 9B**). However, at -20 °C a small shoulder appeared on the low field region, possibly due to binding of **10** to the abasic site (**Figure 9C**). When the temperature was further reduced to -30 °C, the slow-moving shoulder increased and the fast-moving component decreased, indicating increased binding of the spin-label **10** to abasic site DNA (**Figure 9D**).

The cytosine derivative of the 5-alkyne-linked spin-label was measured in the presence of a 14-mer duplex DNA with guanine as the basepairing partner (**Figure 9**). Small slow-motion component immediately appeared as a shoulder, in the low field region, at 0 °C and as a small dent in the high field reagion (**Figure 9E**). Decreasing the temperature the fast-moving component decreased both at high- and low-field region with increasing slow moving components (**Figure 9F,G,H**). After decreasing the temperature to -30 °C the fast-moving component had almost disappeared, leaving a small peak on top of the slow-moving component (**Figure 9H**). This indicates that the spin label **11** is almost fully

bound to the abasic site in duplex DNA. 4-amino-linked spin-label showed no slow-moving components, even at -30 °C **(Figure 9I-L)** indicating that spin label **12** does not bind to the abasic site in duplex DNA.

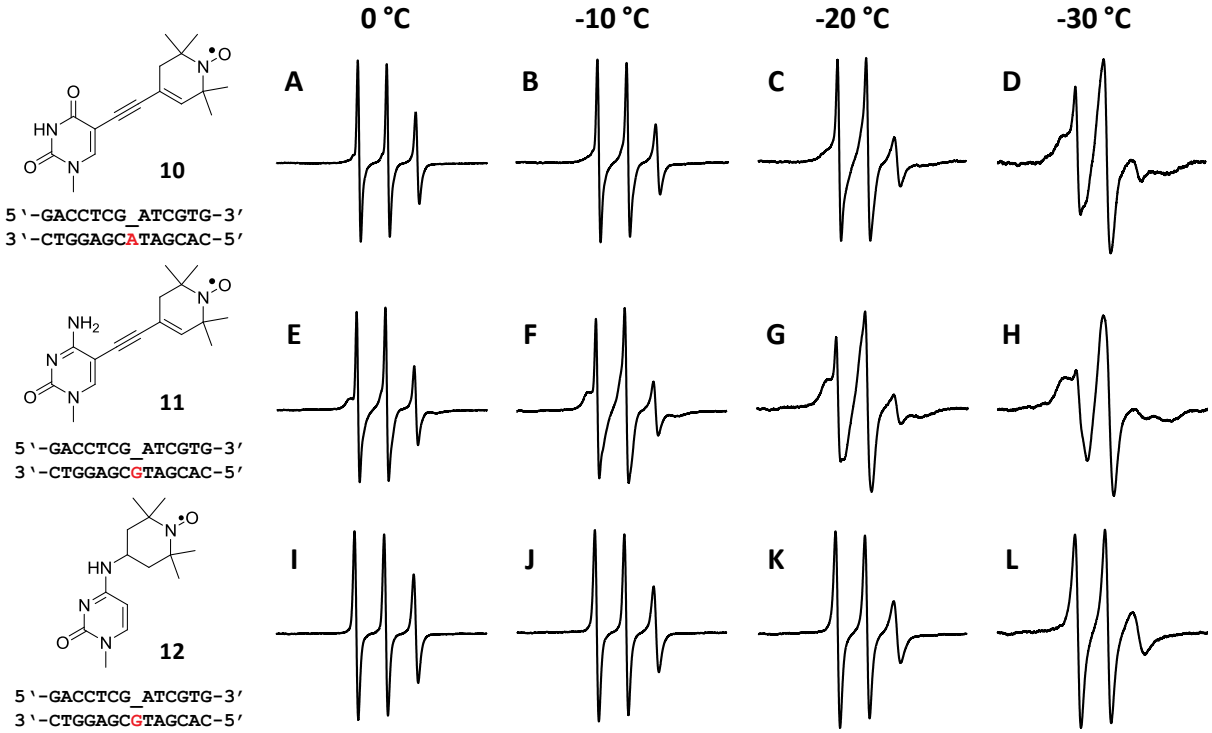

Figure 9. EPR spectra of simple pyrimidine derived spin-labels in a solution containing abasic site duplex DNA. All measurements were conducted in a phosphate buffer containing 30% aqueous ethylene glycol solution and 2% DMSO. **A-D**. Spectra of uracil derived 5-alkyne-linked spin-label **10** at 0, -10, -20, -30 °C, respectively. **E-H**. Spectra of cytosine derived 5-alkyne-linked spin-label **11** at 0, -10, -20, -30 °C, respectively. **I-L**. Spectra of cytosine derived 4-amino-TEMPO spin-label **12** at 0, -10, -20, -30 °C, respectively.

2.3.2 Binding of spin labels 10, 11 and 12 to RNA

Binding of the spin labels **10**, **11** and **12** to an abasic site in duplex RNA, having guanine as orphan base, was also investigated. None of the spin labels showed any binding at -30 °C indicating that these labels are not suitable for noncovalent RNA labeling **(Figure 10)**. These results are not that surprising because RNA forms an A-form helix which has much narrower major groove than B-form DNA.

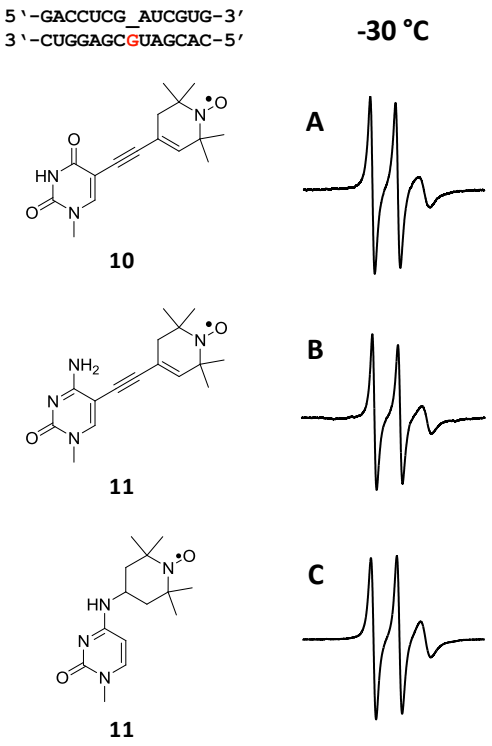

Figure 10. EPR spectra of simple pyrimidine-derived spin labels in a solution containing abasic site duplex RNA. All measurements were conducted in a phosphate buffer containing a 30% aqueous ethylene glycol solution and 2% DMSO. **A**. Spectrum of uracil derived 5-alkyne-linked spin label **10** at -30 °C. **B**. Spectrum of cytosine derived 5-alkyne-linked spin label **11** at -30 °C. **C**. Spectrum of cytosine derived 4-amino-TEMPO spin label **12** at -30 °C.

2.3.3 Determination of binding affinity

The EPR spectra of spin labels **10** and **11** and the spectra of the spin labels containing an abasic site duplex DNA at -30 °C were normalized by double-integrating their values in MATLAB-based program to get a normalized spectra. Since there was no fully bound spectrum, a fully bound spectrum was simulated and used to fractionally subtract from unbound spectrum. The simulated spectrum was subtracted from the unbound spectra on the same graph by adjusting the faction value α to get the visual best-fit. Dissociation constant (k_d) was calculated by inserting α into the following equation:

$$K_{eq} = \frac{(1-\alpha) \times X}{[Y-(1-\alpha) \times X][\alpha \times X]}$$

and K_d = 1/Keq, were X and Y are initial concentrations of spin label in abasic site DNA.

Since there were some problem with normalization of the spectra we were unable to get an accurate dissociation constant (k_d) so binding was drawn from α and determined that spin label **10** bound ca. 30% and spin label **11** ca. 90%.

2.4 Modeling spin-labels in abasic site nucleic acids

To understand the binding of spin-labels in abasic site, they were modeled in duplex DNA that contains an abasic site and minimized to the lowest energy state. That should give the most likely conformation of the spin label in the abasic site in duplex DNA. Though rotation along the single bond does not require much energy, the orientation of the tetrahydropyridine towards the pyrimidine be in any conformation without affecting the binding.

The cytosine-derived, triazole-linked spin label **3** twists a little due to the intramolecular hydrogen bonding (**Figure 11B**), which affects the stacking ability of the label (**Figure 12B**). It appears that the twisting effect in spin-label **3** overcomes the gain of extra hydrogen bonding.

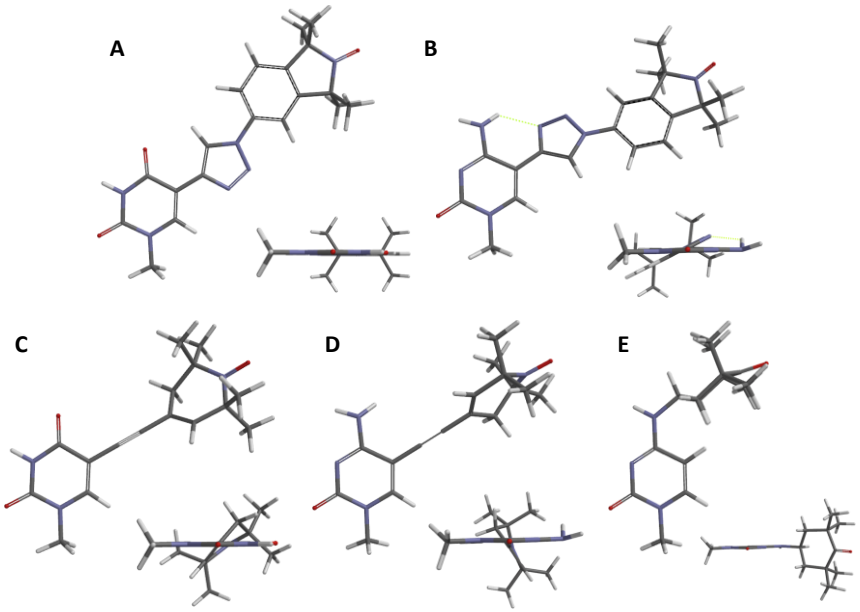

Figure 11. Structures of simple pyrimidine-derived spin labels in the lowest energy state shown in side- and top view for each label. **A**. Uracil derived 5-triazole-linked spin-label **2**. **B**. Cytosine derived 5-triazole-linked spin label **3**. **C**. Uracil-derived 5-alkyne-linked spin label **10**. **D.** Cytosine derived 5-alkyne-linked spin label **11**. **E**. Cytosine derived 4-amino-TEMPO spin-label **12**.

The 5-alkyne-linked spin-labels **10** and **11** and 4-amino-linked spin-label **12** were minimized to their lowest energy state. There we can see that the modifications on the pyrimidines all twist out of plane which can interfere with the binding due to steric hindrance (**Figure 11C-E**). When the labels where modeled in nucleic acid, very similar conformations were seen. The alkyne linked labels stick far out into the major groove and there is no indication that the methyl groups of the tetrahydropyridine moiety crashes into the backbone (**Figure 12C and D**). There is a significant difference in binding between the cytosine and the uracil derivatives, and because the alkyne linked labels do not stack well most binding is through hydrogen bonding. Since cytosine forms three hydrogen bonds compared to uracil's two hydrogen bonds we can assume that binding is increased due to additional binding of the hydrogen bonds.

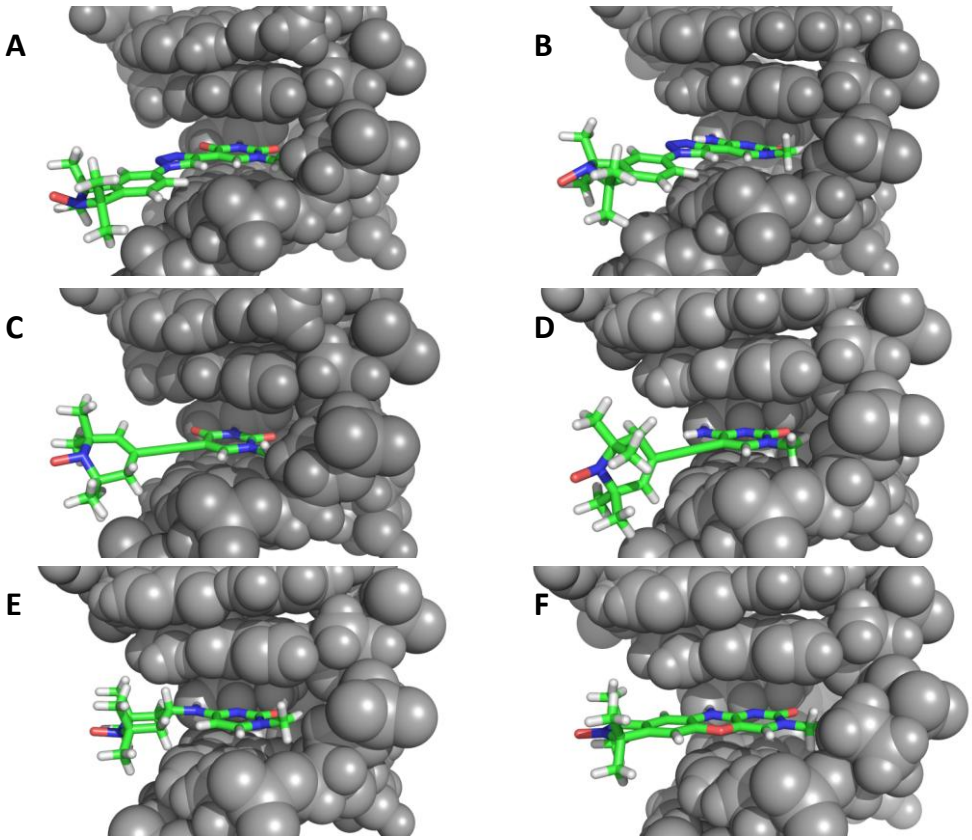

Figure 12. Models of spin-labels in 5-mer nucleic acids with matching orphan base pair. **A**. Uracil derived 5-triazole-linked spin label **2**. **B**. Cytosine derived 5-triazole-linked spin label **3**. **C**. Uracil derived 5-alkyne-linked spin label **10**. **D**. Cytosine derived of 5-alkyne-linked spin label **11**. **E**. Cytosine derived 4-amino-TEMPO **12**. **F**. **ç**.

Minimization of 4-amino-linked spin-label shows that the TEMPO does not stick out long enough for it to get free rotation, hence it crashes into the nucleic acid backbone (**Figure 12E**). That explains why the label does not bind to the abasic site pocket.

2.5 Spin-labels with higher affinity for abasic sites

From the EPR data of spin labels **10**, **11**, **12** (**Figure 9**), it appears that they do not have high enough binding affinity. Unmodified purines with high affinity toward abasic sites in duplex DNA have been described by Lhomme et al. Lhomme used a polyamine linker, coupled to an intercalator, to bind an otherwise unmodified adenine noncovalently with high affinity to an abasic site in duplex DNA (**Figure 13**) [27, 29]. The adenine was used to direct the binding specifically to the abasic site. The polyamine linker, which is protonated at neutral pH giving it a positive charge, was linked to the purine. The positively charged polyamine linker formed ionic bonds to the polyanionic backbone of the nucleic acid, thereby increasing its binding affinity. For additional binding a known intercalator, acridine, was coupled to the linker. Intercalators, like acridine, stack in-between the bases, thus increasing the binding affinity.

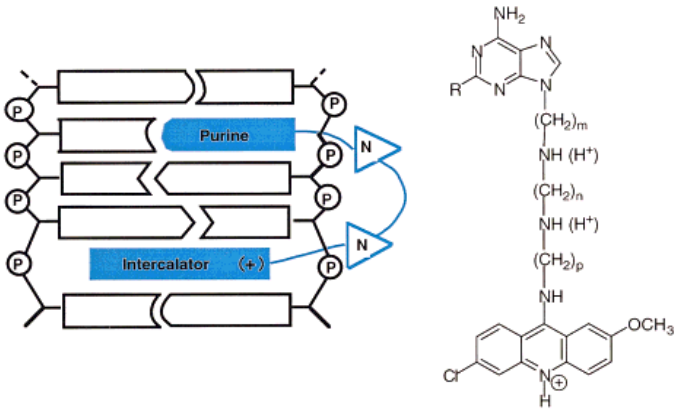

Figure 13. Method developed by Lhomme for increased noncovalent binding affinity [29].

We wanted to utilize this method for our spin-labels, hoping it would give high affinity towards an abasic site in duplex DNA. Since an eleven atom linker, containing three amines coupled to acridine, had the best affinity [27], we chose that linker for the target spin labeled molecule (**Figure 14**).

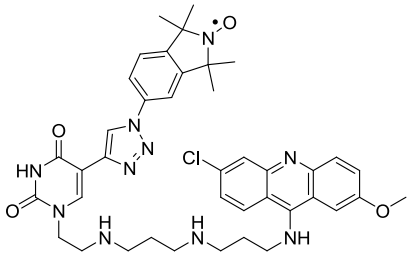

22

Figure 14. Structure of the proposed spin label **22** containing a polyamine linker and acridine to incease the affinity for abasic site.

A scheme was proposed based on Lhomme's synthetic route [27] (**Scheme 6**). The main difference was that we used uracil as starting material. The linker can be coupled to the uracil with and without the acridine attached, giving two options. Spin label modification on the pyrimidine was to be synthesized after attaching the linker and acridine.

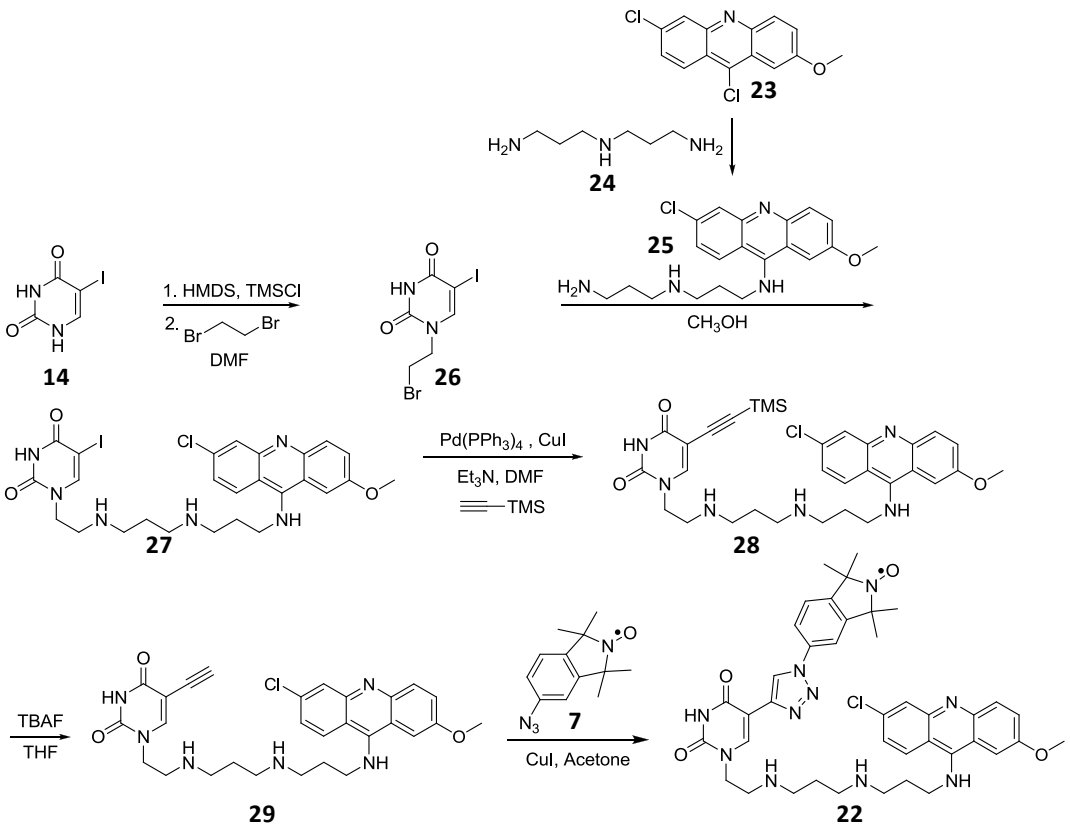

Scheme 6. A proposed synthetic route for **22** based on Lhomme's method.

After devising the scheme, we proceeded with the synthesis. Coupling of free linker to acridine was performed without solvent having the linker in 20 fold excess, giving **25** in reasonable yield (**Scheme 7**).

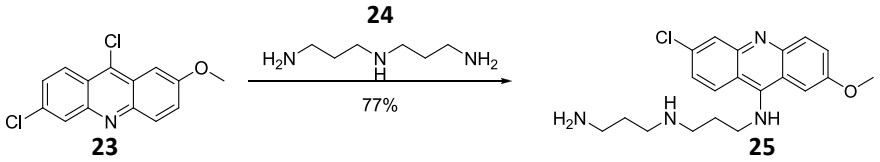

Scheme 7. Synthesis of **25**.

Alkylation of **14** with 1,2-dibromoethane in DMF was performed on the N1 of the pyrimidine using silyl protecting groups for the carbonyl as before (**Scheme 8**). The reaction gave low yield, presumably due to unwanted side products like dialkylation, dimerization and intramolecular cyclizations.

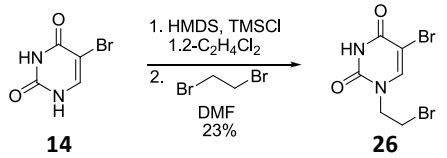

Scheme 8. Synthesis of **26**.

Next step was to couple the linker to the alkyl bromide modified uracil (**Scheme 9**). The reaction was performed with excess linker **24** in methanol until a new product precipitated. The precipitate was analyzed and concluded to be compound **30** where the linker worked as a base to catalyze

intramolecular cyclization (**Scheme 9**). The crude reaction mixture was analysed as well, giving a very unclean NMR. However, there were some indications that some of the desired product **31** was in the reaction mixture. The NMR showed some peak shift correlating to the wanted compound. The assumption came from peaks with similar coupling constant as the free polyaminolinker **24** and similar shift as **25** (NMR of compound **31**). Nevertheless, it was impossible to verify due to low signal compared to linker and other impurities in the baseline. When we attempted to purify the product, it turned out to be very polar and difficult to isolate from linker **24**, even on silica gel treated with triethylamine before washing the compound through with 20% methanol in dichloromethane.

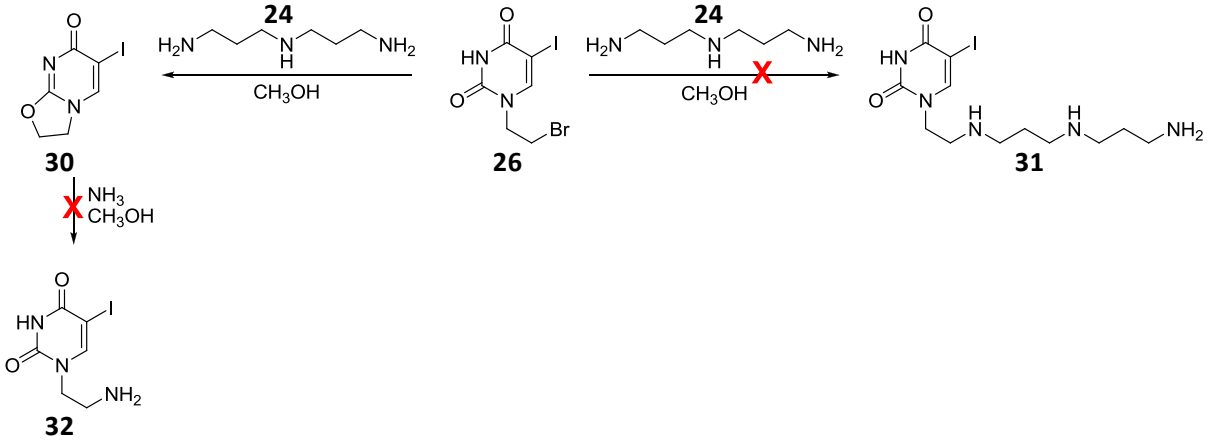

Scheme 9. Intramolecular cyclization as side reaction.

Ring opening reactions of compound **30** were attempted with no luck. Although many other reaction conditions were attempted, like different temperatures, solvents and reagent equivalence, the isolation of product **31** remains in vain.

After a futile effort for many months, this approach was discarded and a new approach planned. The new approach proposed uses reductive amination to couple the linker to the modified base (**Scheme 10**). This approach should circumvent the intramolecular cyclization. Another change was also proposed in the new scheme due to the problems in purifying the polyamine linker compound. The addition of the linker was moved to the end of the scheme so there will be only one compound containing the polyamine linker to purify. This means that we start by coupling the aldehyde to the base followed by the Sonogashira coupling. Deprotection will then be done prior to the final two steps of click reaction and reductive aminaiton, which will give the target spin-label **22**.

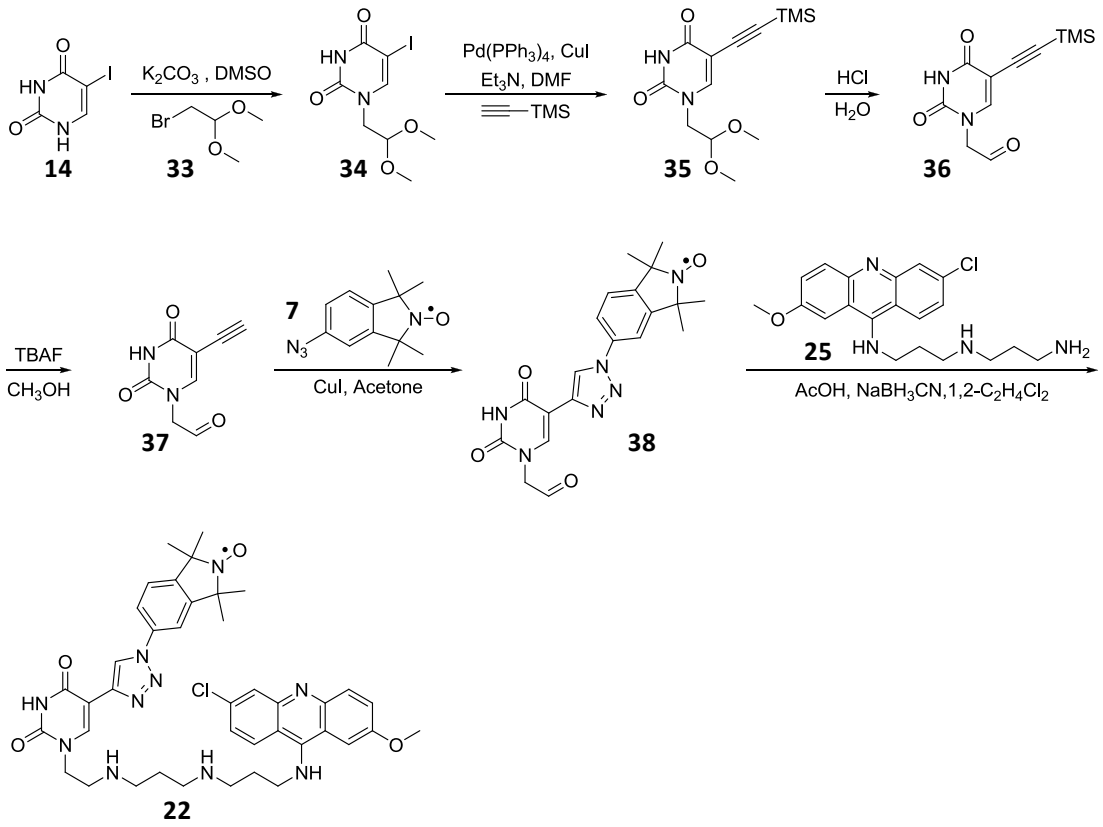

Scheme 10. New proposed synthetic route for **22**.

The alkylation of **14** presented some problems; silyl protection did not yield a product so potassium carbonate was exploited in presence of DMSO and the 2-bromo-1,1-demethoxyethane (**33**). No reaction was observed at low temperature although upon heating regioselectivity diminished giving only dialkylation. Microwave irritation was utilized and gave the monoalkylation in very low yield. Finally we came up with the method of making the uracil salt by stirring the potassium carbonate in DMSO charged with uracil, before adding the alkyl halide. This method awarded the monoalkylated compound **34** in 60% yield (**Scheme 11**). Sonogashira coupling was subsequently performed on the monoalkylated uracil **34** giving compound **35** in moderate yield (**Scheme 11**).

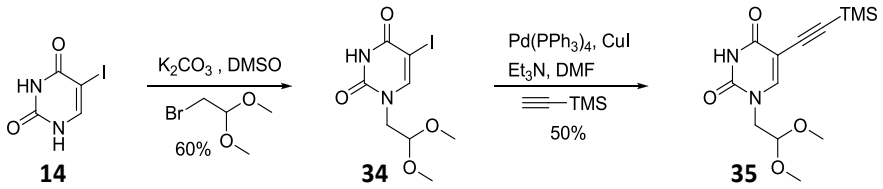

Scheme 11. Synthesis of **32** and **33** from 5-iodo-uraci **14**.

The next step was to deprotect the acetal and TMS group. One step deprotection was tried since mild acidic conditions can be used for deprotection of the acetal and halogens are known to remove silyl groups **(Sceme 12)**. To our surprise, the acetal remained unchanged but the TMS group was removed, making way for Markonikov addition of the hydrochloric acid to yield **39** (**Scheme 12**). The structure of compound **39** was confirmed with mass spectrometry and DEPT NMR spectroscopy, was utilized by determining the number of proton on each carbon. Normal proton and carbon NMR was also used. Upon further heating, the acetal formed hemiacetal which is ready for reductive aminaiton. Since the Markonikov product cannot be used further, another approach was proposed.

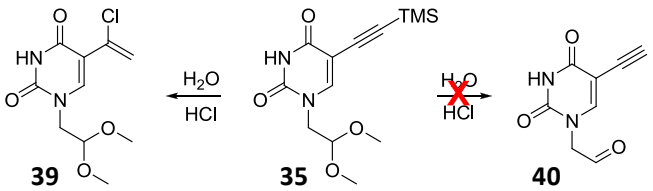

Scheme 12. 35 reacted with 0.1 M HCl.

In the new scheme we started by alkylating uracil **14** like before, followed by Sonogashira coupling of TMS acetylene, yielding **35**. The TMS group was removed with TBAF, giving acetylene **36** ready for click reaction with the azide spin-label **7**. Click reaction was performed on **41** in presence of copper iodide which gave **44** in good yield. Acetal will then be deprotected and reductive ammination performed to give the target molecule **22 (Scheme 13)**.

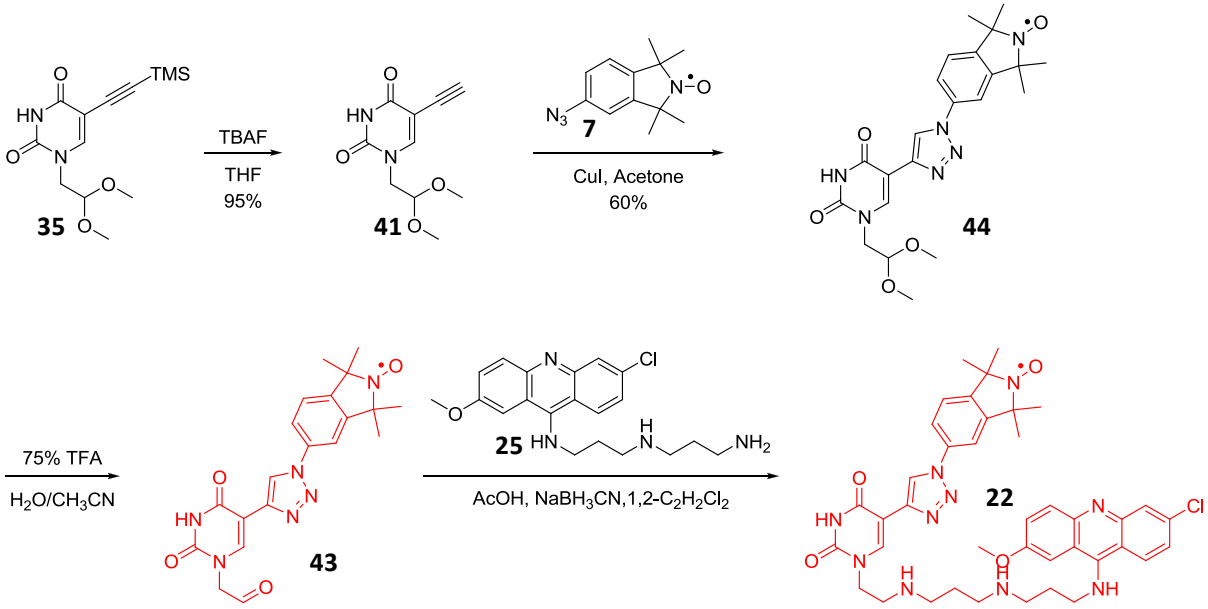

Scheme 13. The current synthetic route and status of the synthesis towards **22**. Red compounds are yet to be made.

We were also able to deprotect the acetal **32**, which gives hemiacetal **45** in equilibrium with the aldehyde **44**. So far there has been no luck performing reductive ammination with the model compound propylamine **(Figure 14)**.

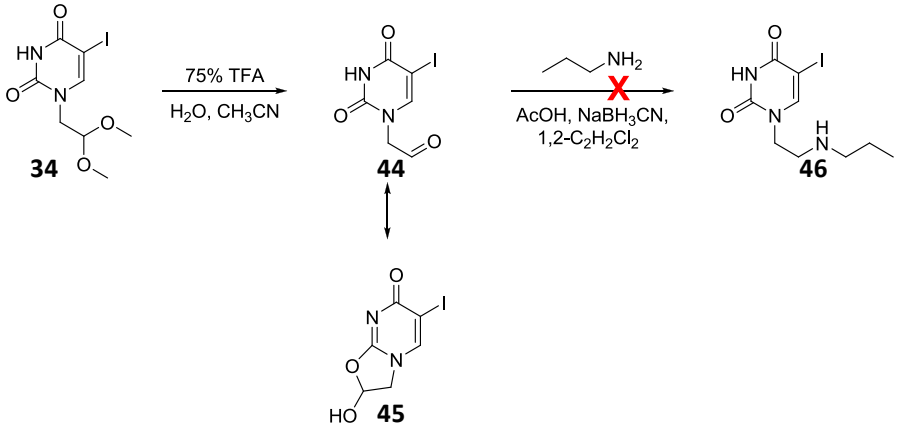

Scheme 14. Acetal deprotection of **34** and failed reductive ammination with propylamine.

In conclusion, synthesis of a polyamine-conjugated spin label has caused problems due to many reactive sites which lead to intramolecular cyclization and low yield in alkylation. Addition and purification of the polyamine linker are still in progress

3 Summary

I have described the synthesis of three new spin labels for noncovalent and site-directed spin labeling and determined how well they bind to abasic sites in duplex DNA and RNA. Two spin-labels were 5-alkyne-linked pyrimidine derivatives and one was a cytosine derivative linked with 4-amino-TEMPO. 5-alkyne-linked labels **10** and **11** showed ca. 30% and 90% binding to abasic site DNA, respectively but no binding in RNA. 4-amino-linked cytosine showed binding in neither DNA nor RNA.

A molecule for high affinity noncovalent binding to abasic site duplex DNA was proposed by attaching polyamine linker coupled to an acridine, a known intercalator, to a spin-label. There were some problems in the synthetic route of the molecule due to intramolecular cyclization and low yielding steps. Nevertheless, a solution has been synthesized and will be measured in abasic site DNA in near future.

4 Experimental

General

All commercially available reagents were purchased from Sigma-Aldrich and used directly. Solvents purchased from Sigma-Aldrich or Skeljungur hf were dried, when needed, with molecular sieves (3A, 1.6 mm pallets) or by distillation. Thin layer chromatography (TLC) plates, with glass back were purchased from Silicycle (Kieselgel 60 F254, 250µm). For flash column chromatography, silica gel (230-400 mesh, 60 Å), was purchased from Silicycle and used directly. NMR studies were preformed on a Bruker Avance 400 MHz using deuterated solvents d_6-DMSO (2.50 ppm), d_4-CH_3OH (3.35 and 4.78 ppm) and d-$CHCl_3$ (7.26 ppm). HR-APCI-MS (Bruker, MicroTof-Q) mass spectrometer was used to record molecular mass of organic compounds.

DNA synthesis and purification

CPG columns and solutions for DNA synthesis were bought from ChemGenes corporation. Oligonucleotides, both unmodified and modified, were synthesized on an automatic ASM800 DNA synthesizer (Biosett) using a trityl-off synthesis protocol and phosphoramidites with standard protecting groups on 1.0 µmol scale. DNA protection groups were deprotected using conc. ammonia solution at room temperature and cleaved from the resin at 55 °C for 8 h. DNA oligos were purified by 20% denatured polyacrylamide gel electrophoresis (DPAGE) and visualized under UV. A band was isolated, crushed and extracted with TEN buffer (259 mM NaCl, 10 mM Tris, 1 mM Na_2EDTA; pH 7.5). Extracts were filtered through 0.45 µm polyethersulfone membrane from Whatman and desalted using Sep-Pak cartridge from Waters Corporation. Solvent was removed in Speed-Vac and the residue was re-dissolved in 200 µL of sterile water. Concentration was measured on UV Winlab (V2.85.04, PerkinElmer) using Beer's law calculations based on absorbance at 260 nm.

EPR measurements

Solution of spin-label, DNA strand and complimentaty strand (1:2:2.4) were mixed, stirred and solvent evaporated on Speed-Vac. The residue was dissolved in 10 µL PNE buffer (10 mM Na_2HPO4, 100 mM NaCl, 0.1 mM Na_2EDTA, pH 7) and annealed (Annealing protocol: 90 °C for 2 min, 60 °C for 5 min, 50 °C for 5 min, 40 °C for 5 min, 22 °C for 15 min). Solvent was again dried on Speed-Vac before dissolving in 10 µL of 30% ethylene glycol water solution containing 2% DMSO for solubility. Solution was placed in 50 µL capillary (BLAUBRAND intraMARK). The EPR spectra were recorded using a minimum of 25 scans up to 250 on a MiniScope MS 200 (Magnettech Germany) EPR spectrometer (100 kHz modulation frequency, 1.0 G modulation amplitude, and 2.0 mW microwave power).

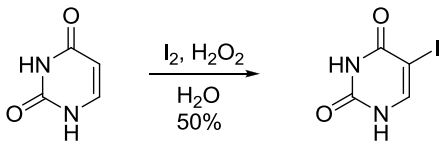

13 **14**

5-iodopyrimidine-2,4(1H,3H)-dione (14). Uracil **13** (5 g, 44,6 mmol) and I_2 (6,5 g 25,6 mmol) were suspended in water (140 mL) and 30% H_2O_2 (6 mL) was added. The resulting reaction mixture was stirred at 50 °C for 12 h. Reaction mixture was allowed to cooled to 25 °C. The precipitate was filtered and washed with water and aqueous Na_2S2O_3 solution giving **14** (5.04 g, 21.2 mmol) as white crystals in 47% yield. [30]

TLC: 10% CH_3OH:CH_2Cl_2 R_f(**13**) = 0.2 R_f(**14**) = 0.5

^{1}H NMR (400 MHz, d_6-DMSO) δ ppm 11.39 (s, 1H, NH), 11.19 (s, 1H, NH), 7.89 (s, 1H, H)

^{13}C NMR (d_6-DMSO) 161.56, 151.31, 147.04 67.67

Mass (M+Na) calculated: 260.9131 Mass (M+) found: 260.9124 err: 2.9 ppm

Notbook ref: GBSI-281, 195, 39, 35 and GBSII-49

NMR ref: GBSI-35

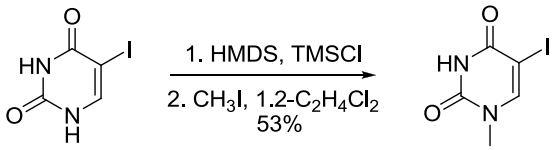

14 **15**

5-iodo-1-methylpyrimidine-2,4(1H,3H)-dione (15). To a suspension of 5-iodo-Uracil **14** (800 mg, 3.36 mmol) in 1,2-dichloroethane (10 mL), HMDS (2.0 mL, 8.4 mmol) and TMSCl (0.2 mL, 1.7 mmol) were added and refluxed for 3 h under argon atmosphere. Reaction mixture was cooled to 50 °C, solvent and excess silyl reagents were distilled out under reduced pressure. Fresh 1,2-dichloroethane (10 mL) and CH_3I (0.8 mL) were added followed by I_2 (10 mg) as catalyst and reaction mixture refluxed for 24 h. Solvent was removed under high vacuum and purified by column chromatography CH_3OH:CH_2Cl_2 0:100 →4:96 giving **15** (205.5 mg, 0.815 mmol) as white crystals in 24% yield.

TLC 5% CH_3OH in CH_2Cl_2 R_f(**15**)=0,5 R_f(**14**)=0.3

^{1}HNMR (400 MHz, d_6-DMSO) δ ppm 11.59 (s, 1H NH), 8.18 (s, 1H, H5), 3.23 (s, 3H, CH3)

^{13}CNMR 160.89, 150.68, 150.43, 67.05, 34.56

Mass (M+Na) calculated: 274.9288 Mass (M+Na) found: 274.9341 err: 19 ppm

Notebook ref: GBSI- 225 and 197

NMR ref: GBSI-225-1

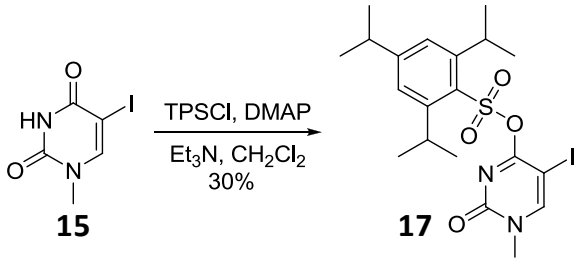

15 **17**

5-iodo-1-methyl-2-oxo-1,2-dihydropyrimidin-4-yl 2,4,6-triisopropylbenzenesulfonate (17). Compound **15** (435.2 mg, 1.72 mmol), TPSCl (362.2 mg, 2.40 mmol) and DMAP (19.1 mg, 0.156 mmol) were dissolved in anhydrous CH_2Cl_2 (5.5 mL) at 0°C and Et_3N (0.2 mL) added. The resulting reaction mixture was stirred for overnight at 23°C and diluted with CH_2Cl_2, and washed with water, aqueous $NaHCO_3$ and brine. Organic layer was dried over Na_2SO_4 and solvent was removed in vacuo. The residue was isolated by column chromatography using Ethyl acetate: petroleum (10:90 → 30:70) to give compound **17** (264.9 mg, 0.527 mmol) as white solid in 30% yield.

TLC: 25% ethyl acetate:petroleum ether or 5% CH_3OH:CH_2Cl_2 R_f(**17**)=0.8 R_f(**15**)=0.2

^{1}HNMR (400 MHz, d-$CHCl_3$) δ ppm 7.85 (s, 1H, H5), 7.20 (s, 2H, Hb), 4.30 (td, J = 13.50, 6.74, 6.74 Hz, 2H Hd), 3.45 (s, 3H, CH_3), 2.90 (td, J = 13.82, 6.91, 6.91 Hz, 1H, Hc), 1.30 (d, J = 6.75 Hz, 12H, o-CH_3), 1.25 (d, J = 6.91 Hz, 6H, p-CH_3)

^{13}CNMR not recorded, unstable

Mass (M+Na) calculated: 541.0634 Mass (M+Na) found: mass not found, unstable

Notebook ref: GBSI-271

NMR ref: GBSI-271-2

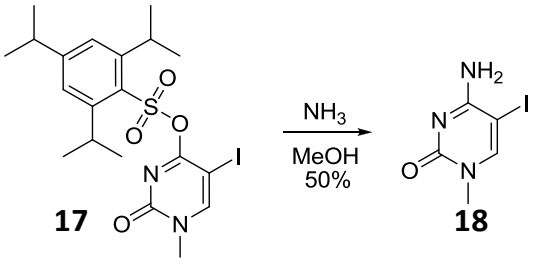

17 **18**

4-amino-5-iodo-1-methylpyrimidin-2(1H)-one (18). Compound **17** (256.8 mg, 0.511 mmol) was dissolved in conc. NH_3 in methanol (10 mL) and stirred for 7 h. Reaction mixture was diluted with CH_2Cl_2 and washed with water, $NaHCO_3$ and brine. Organic layer was dried over Na_2SO_4 and solvent removed in vacuo. Residue was purified by column chromatography CH_3OH:CH_2Cl_2 (0:100 → 5:95) giving **18** (63.7 mg, 0.254 mmol) as white solid in 50% yield.

TLC: 10% CH_3OH:CH_2Cl_2 R_f(**17**)=0.9 R_f(**18**)=0.2

^{1}HNMR (400 MHz, d_6-DMSO) δ ppm 8.08 (s, 1H, H5), 7.58 (s, 1H, NH), 6.42 (s, 1H, NH), 3.22 (s, 3H, CH_3)

^{13}CNMR 163.18, 154.85, 152.27, 54.51, 36.17

Mass (M+Na) calculated: 251.9628 Mass (M+Na) found: 251.9626 err: 0.9 ppm

Notebook ref: GBSI-273

NMR ref: GBSI-273

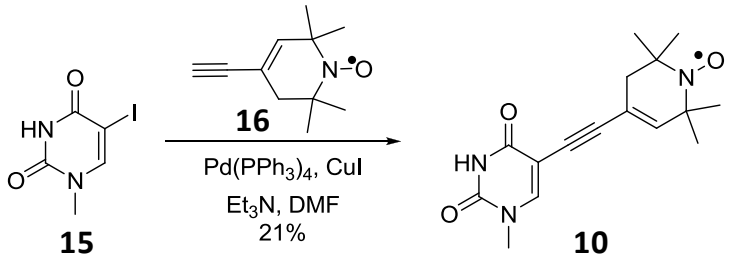

Compound 10. Compound **15** (10 mg, 0.0397 mmol) and spin-label **16** (11.2 mg, 0.0628 mmol) were dissolved in DMF (0.5 mL) and argon bubbled through. $Pd(PPh_3)_4$ (3.6 mg, 0.0031 mmol) and CuI (1 mg, 0.005 mmol) were added along with Et_3N (10 µL). Argon was bubbled through again and stirred at 50°C for 3 h. The resulting reaction mixture was diluted with CH_2Cl_2 (24 mL) and washed with water (2x30 mL), aqueous $NaHCO_3$ (2x10 mL) and brine (20 mL). Organic layer was dried over Na_2SO_4 and solvent removed in vacuo. Product was purified on Prep-TLC using 4% CH_3OH in CH_2Cl_2 and giving product **10** (2.5 mg, $8.3x10^{-3}$ mmol) at R_f = 0.2 as yellowish solid in 21% yield.

TLC: 5% CH_3OH:CH_2Cl_2 R_f(**15**)=0.1 R_f(**10**)=0.5

Mass calc (M+Na): 325.14 Mass found (M+Na): 325.1397 err = 4.6 ppm

Notebook ref: GBSI-265

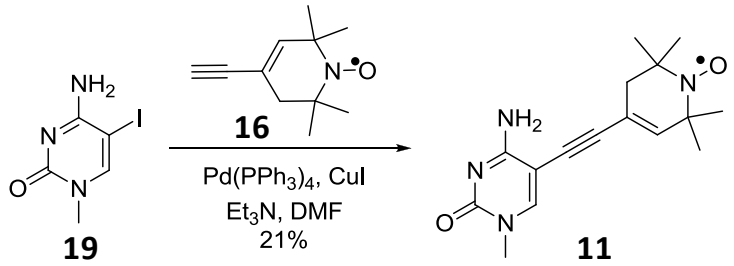

Compound 11. Compound **19** (10.2 mg, 0.0406 mmol) and spin-label **16** (9.1 mg, 0.0511 mmol) were dissolved in DMF (0.5 mL) and argon bubbled through. $Pd(PPh_3)_4$ (3.0 mg, 0.0026 mmol) and CuI (1 mg, 0.005 mmol) were added along with Et_3N (10 µL). Argon was bubbled through again and stirred at 50°C for 2 h. The resulting reaction mixture was diluted with CH_2Cl_2 (24 mL) and washed with water (2x30 mL), aqueous $NaHCO_3$ (2x10 mL) and brine (20 mL). Organic layer was dried over Na_2SO_4 and solvent removed in vacuo. Product was purified on Prep-TLC using 10% CH_3OH in CH_2Cl_2 giving product **11** (2.6 mg, $8.6x10^{-3}$ mmol) at R_f = 0.3 as yellowish solid in 21% yield.

TLC: 10% CH_3OH:CH_2Cl_2 R_f(**19**)=0.2 R_f(**11**)=0.5

Mass calc (M+H): 302.1737 Mass found (M+H): 302.1755 err = 6.0 ppm

Mass calc (M+Na): 324.1557 Mass found (M+Na): 324,1565 err = 2.5 ppm

Notebook ref: GBSI-275, GBSI-251

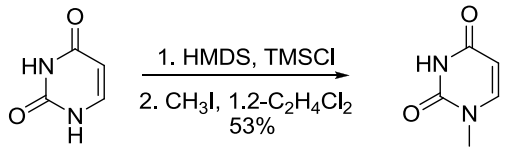

13 **19**

1-methylpyrimidine-2,4(1H,3H)-dione (19). To a suspension of uracil **13** (0.500 g, 4.46 mmol) in 1,2-dichloroethane (10 mL), HMDS (3.8 mL, 18.1 mmol) and TMSCl (0.3 mL, 2.4 mmol) and refluxed for 4 h (or until it clears) under argon atmosphere. Reaction mixture was cooled to 50 °C, solvent distilled out under reduced pressure. Fresh 1.2-dichloroethana (10 mL) and CH_3I (1.1 mL) were added followed by I_2 (5 mg) and refluxed for 24 h. Solvent was removed under high vacuum and purified by column chromatography CH_3OH:CH_2Cl_2 (0:100 → 10:90) giving **19** (256 mg, 2.03 mmol) as white solid in 46% yield.

TLC: 10% CH_3OH: CH_2Cl_2 Rf(**13**) = 0.2 R_f(**19**) = 0,5 R_f(dimethyl) = 0,8

^{1}HNMR (400 MHz, d_6-DMSO) δ ppm 11.21 (s, 1H, NH), 7.61 (d, J = 7.81 Hz, 1H, H4), 5.51 (dd, J = 7.81, 2.29 Hz, 1H, H5), 3.22 (s, 3H, CH_3)

^{13}CNMR 163.78, 151.15, 146.32, 100.40, 35.08

Mass (M+Na) calculated: 149.0321 Mass (M+Na) found: 149.0323 err: 2.5 ppm

Notebook reference: GBSI-133

NMR ref: GBSI-133B

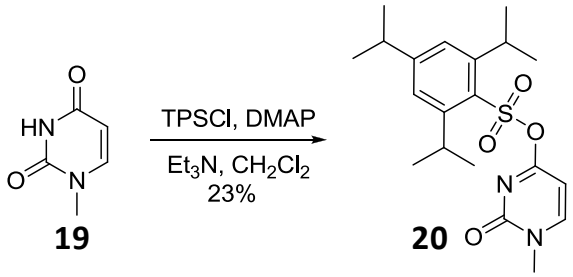

19 **20**

1-methyl-2-oxo-1,2-dihydropyrimidin-4-yl 2,4,6-triisopropylbenzenesulfonate (20). Compound **19** (199.2 mg, 1.579 mmol), TPSCl (360 mg, 2.389 mmol) and DMAP (19 mg, 0.156 mmol) were added to a round bottom flask at 0 °C and dissolved in anhydrous CH_2Cl_2 (6 mL). Et_3N (0.9 mL) was added. The resulting reaction mixture was stirred for 4h at 0 – 20 °C, diluted with CH_2Cl_2 and washed with water, aqueous $NaHCO_3$ and brine. Organic layer was dried over Na_2SO_4 and solvent removed in vacuo. Product was purified by column chromatography CH_3OH:CH_2Cl_2 (0:100 → 4:98) giving **20** (142.5 mg, 0.36 mmol) as white solid in 23% yield.

TLC: 5% CH_3OH:CH_2Cl_2 R_f(**19**)=0.2 R_f(**20**)=0.8

^{1}HNMR (400 MHz, d-$CDCl_3$) δ ppm 7.60 (d, J = 7.04 Hz, 1H, H4), 7.20 (s, 2H, Ar-H), 6.07 (d, J = 7.03 Hz, 1H, H5), 4.24 (td, J = 13.50, 6.75, 6.75 Hz, 2H, He), 3.47 (s, 3H), 2.90 (td, J = 13.79, 6.90, 6.90 Hz, 1H, Hd), 1.27 (dd, J = 13.93, 6.84 Hz, 18H, 6xCH_3)

^{13}CNMR not recorded, unstable

Mass (M+Na) calculated: 415.1667 Mass (M+Na) found: mass not found, unstable

Notebook reference: GBSI-135 NMR ref: GBSI-135A

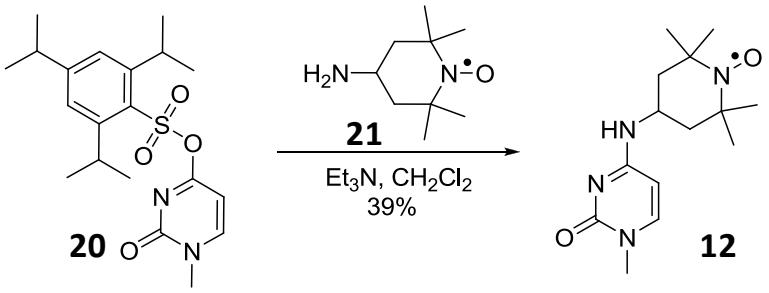

2,2,6,6-tetramethyl-4-(1-methyl-2-oxo-1,2-dihydropyrimidin-4-ylamino)piperidin-1-olate (12). Compound **20** (42.5 mg, 0.108 mmol) and 4-amino-TEMPO (29.6 mg, 0.173 mmol) is dried on high vacuum for 4 h and dissolved in anhydrous CH_2Cl_2 (10 mL) and Et_3N (0.2 mL). The resulting reaction mixture was refluxed for 12 h, diluted with CH_2Cl_2 and washed with water. Organic layer was dried over Na_2SO_4 and solvent removed in vacuo giving **12** (11.9 mg, 0.043 mmol) as white solid in 39% yield.

TLC: 10% CH_3OH:CH_2Cl_2 R_f(**20**) = 0.8 R_f(**21**) = 0 R_f(**12**) = 0.4

Mass calc (M+H): 279.36 Mass found (M+H): 280.18

Mass calc (M+Na): 302.35 Mass found (M+Na): 302.16 err: 11.9

Notebook reference: GBSI-157

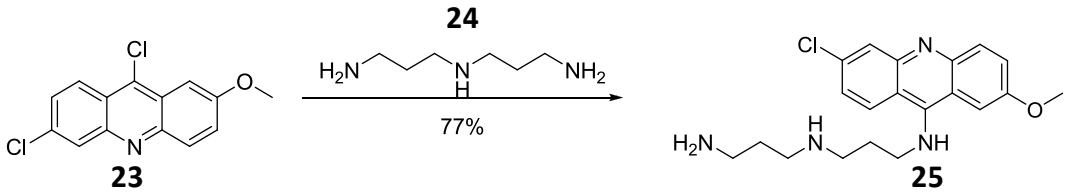

N1-(3-aminopropyl)-N3-(6-chloro-2-methoxyacridin-9-yl)propane-1,3-diamine (25). Acridine **23** (1.4569 g, 5.24 mmol) was dissolved in N1-(3-aminopropyl)propane-1,3-diamine **24** (15 mL, 110 mmol). The resulting reaction mixture was stirred at 70 °C for 2 hours, diluted with CH_2Cl_2 and washed with water (1 L). Organic layer was dried over Na_2SO_4 and solvent removed in vacuo giving **25** (1.50 g, 4.05 mmol) as yellow solid in 77 % yield.

TLC: 10% CH_3OH:CH_2Cl_2 R_f(**23**) = 0.9 R_f(**25**) = 0.1

TLC: 2:15:83 Et_3N:CH_3OH:CH_2Cl_2 Rf(23) = 0.95 R_f(25) = 0.2

^{1}HNMR (400 MHz, CDCl3): δ ppm 8.11 (d, J = 9.29 Hz, 1H), 8.01 (d, J = 2.00 Hz, 1H), 7.96 (d, J = 9.26 Hz, 1H), 7.39 (ddd, J = 9.28, 2.09 Hz, 2H), 7.22 (dd, J = 9.28, 2.09 Hz, 1H), 3.98-3.89 (m, 5H), 2.97-2.93 (m, 2H), 2.81 (td, J = 9.63, 7.02, 7.02 Hz, 4H), 1.90 (td, J = 11.52, 5.86, 5.86 Hz, 2H), 1.79-1.70 (m, 2H)

^{13}CNMR not recorded

Mass (M+Na) calculated: 395.1615 Mass (M+Na) found: not recorded

Notebook ref: GBSI-61 and GBSI-91

NMR ref:

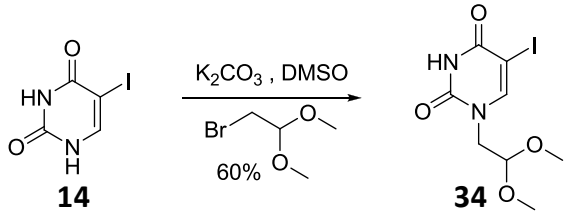

1-(2,2-dimethoxyethyl)-5-iodopyrimidine-2,4(1H,3H)-dione (32). Compound **14** (156,g mg, 0.658 mmol) and K_2CO_3 (92,3 mg, 0.668 mmol) were dissolved in DMSO (6 mL) and stirred at 80°C for 1h. 2-bromo-1,1-demethoxyethane (111,2 mg, 0.658mmol) was added and stirred at 80 °C for 24h. Solvent was removed under high vacuum and purified by column chromatography using Et_3N:CH_3OH:CH_2Cl_2 (4:0:96 → 0:4:96) giving compound **32** (126.2 mg, 0.396) as white solid in 60% yield.

TLC: 5:5:90 Et_3N:CH_3OH:CH_2Cl_2 R_f(**14**)=0.3 R_f(**32**)=0.6

TLC: 60% ethyl acetate : petroleum ether R_f(14)=0.3 R_f(32)=0.6

^{1}HNMR (400 MHz, d_6-DMSO) δ ppm 11.68 (s, 1H), 8.07 (s, 1H), 4.54 (t, J = 5.31, 5.31 Hz, 1H), 3.78 (d, J = 5.33 Hz, 2H), 3.30 (s, 6H)

^{13}CNMR not recorded

Mass (M+Na) calculated: 348.9661 Mass (M+Na) found: not recorded

Notbook ref: GBSI-298 GBSII-53

NMR ref: GBSI-298prep

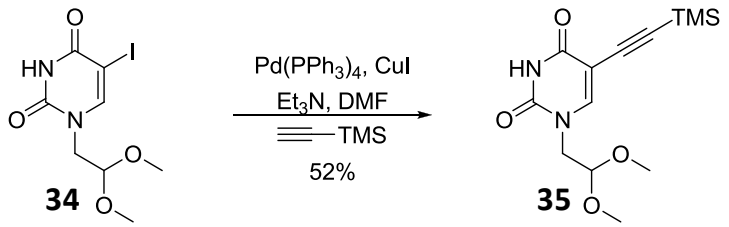

1-(2,2-dimethoxyethyl)-5-((trimethylsilyl)ethynyl)pyrimidine-2,4(1H,3H)-dione (33). Compound **32** (496 mg, 1.52 mmol) and ethynyltrimethylsilane (379.5 mg, 3.87 mmol) were dissolved in DMF and argon bubbled through. $Pd(PPh_3)_4$ (176 mg, 0.152 mmol) and CuI (29 mg, 0.152 mmol) catalysts were added along with Et_3N (230 mg, 2.28 mmol). Argon was bubbled through again. Reaction was stirred at 50°C for 12h, diluted with CH_2Cl_2 and washed with water, aqueous $NaHCO_3$ and brine. Organic layer was dried over Na_2SO_4 and solvent removed in vacuo. Compound was purified by column chromatography using ethyl acetate : petroleum ether (0:100 → 40:60) giving compound **33** (256 mg, 0.863 mmol) as white solid in 57% yield.

Compound was purified on Prep-TLC using 80% ethyl acetate : Petroleum ether

TLC: 80% ethyl acetate : petroleum ether R_f(**33**) = 0.8 R_f(**32**) = 0.7

^{1}HNMR (400 MHz, d_6-DMSO) δ ppm 11.65 (s, 1H, NH), 7.99 (s, 1H, H5), 4.55 (t, J = 5.31, 5.31 Hz, 1H, CH), 3.79 (d, J = 5.31 Hz, 2H, CH2), 3.30 (s, 6H2xCH3), 0.19 (s, 9H, 3xCH3)

^{13}CNMR 161.49, 150.17, 149.61, 100.67, 97.40, 96.87, 96.61, 53.90, 48.53, -0.38

Mass (M+Na) calculated: 319.1090 Mass (M+Na) found: not recorded

Notebook ref: GBSII-47, 81, 89

NMR ref: GBSII-47-1

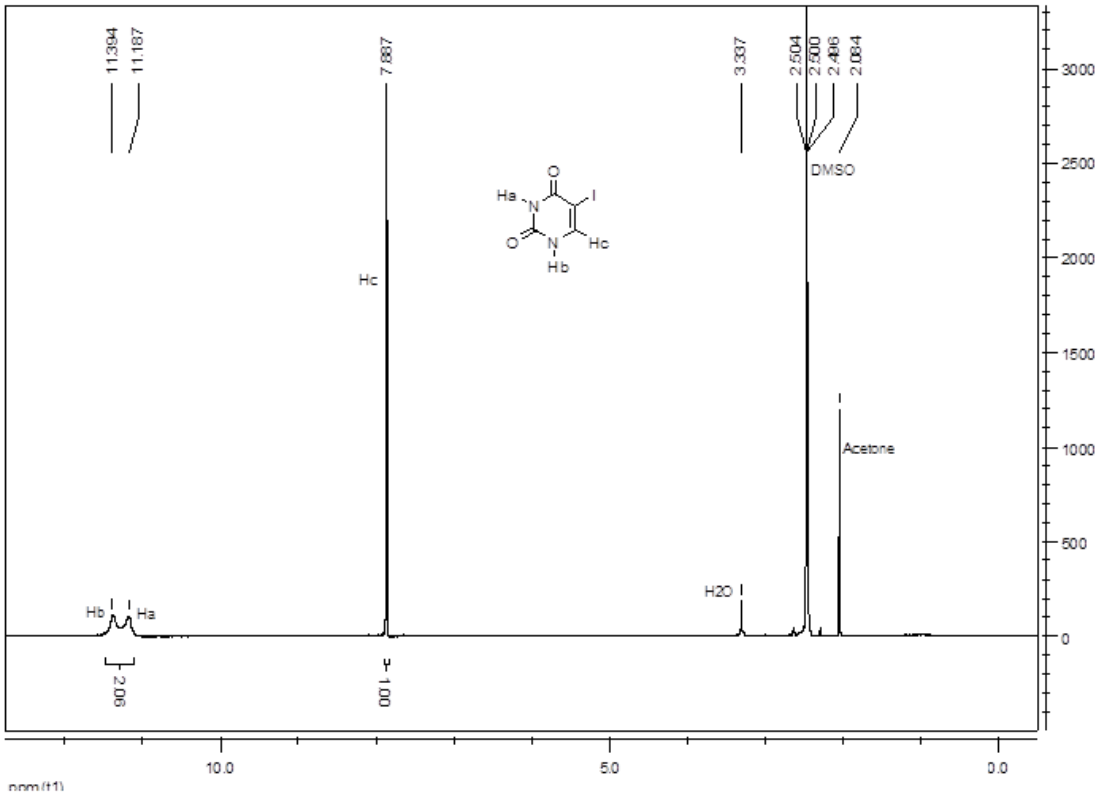

[1]HNMR of compound **14.**

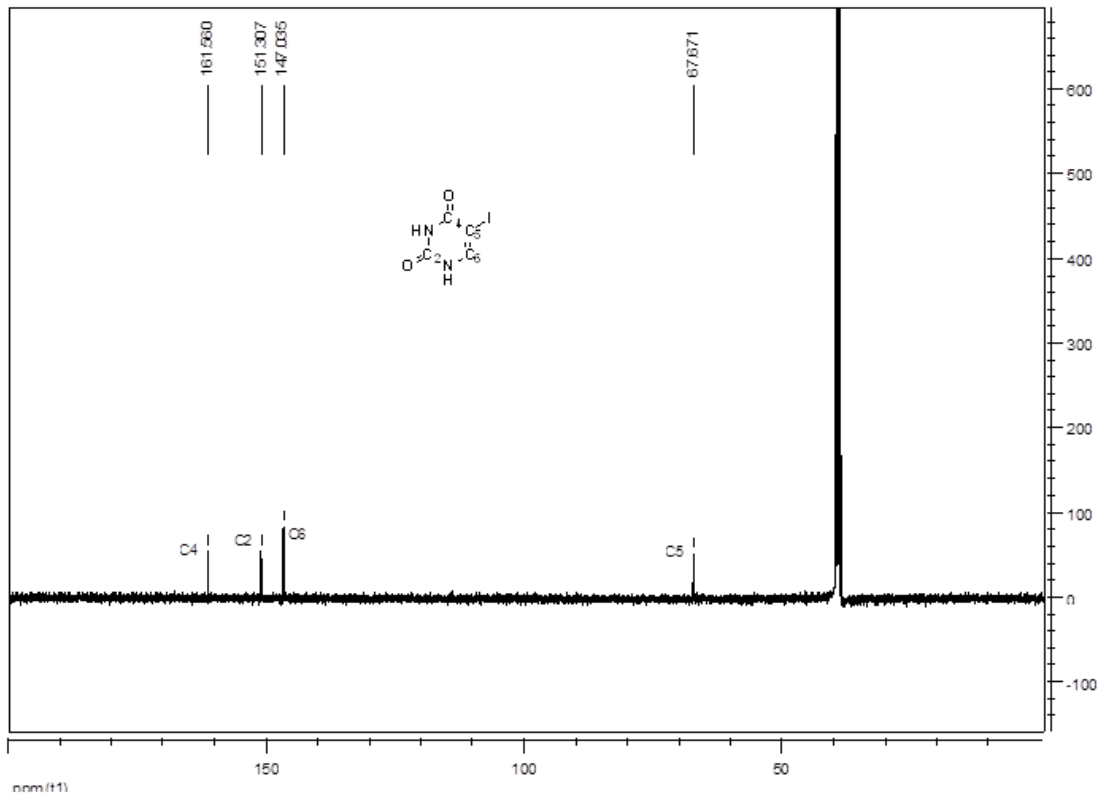

[13]CNMR of compound **14.**

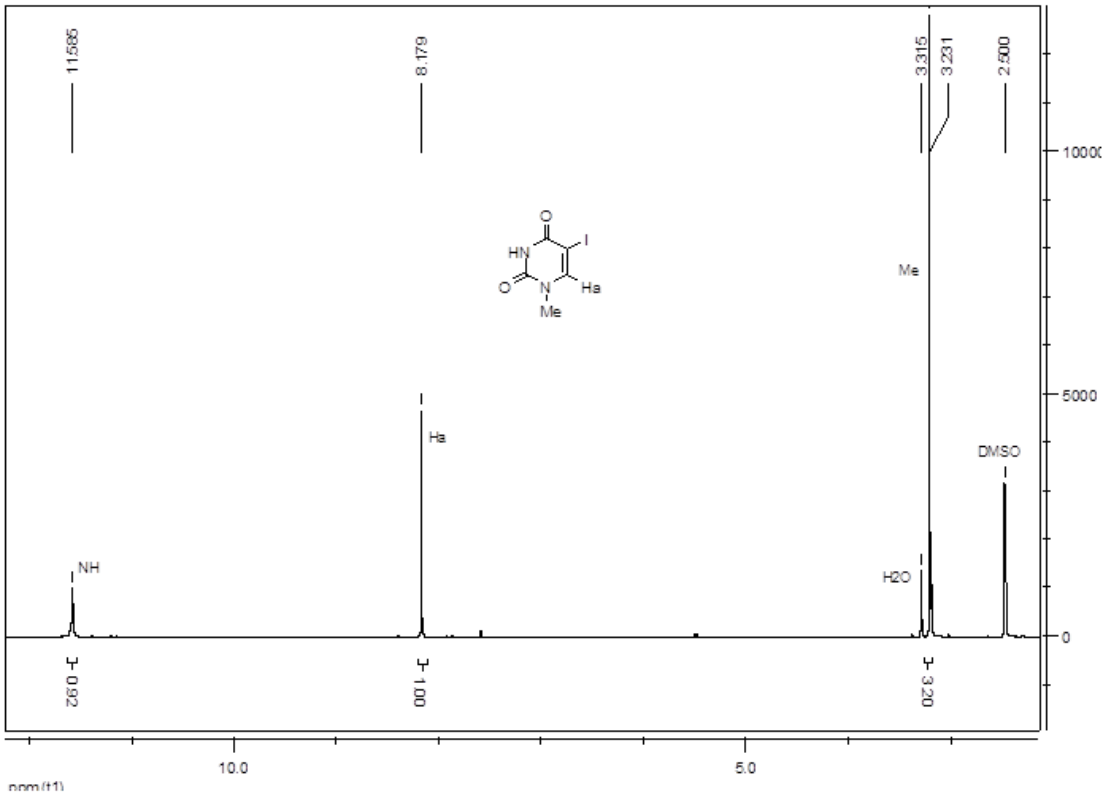

[1]HNMR of compound **15.**

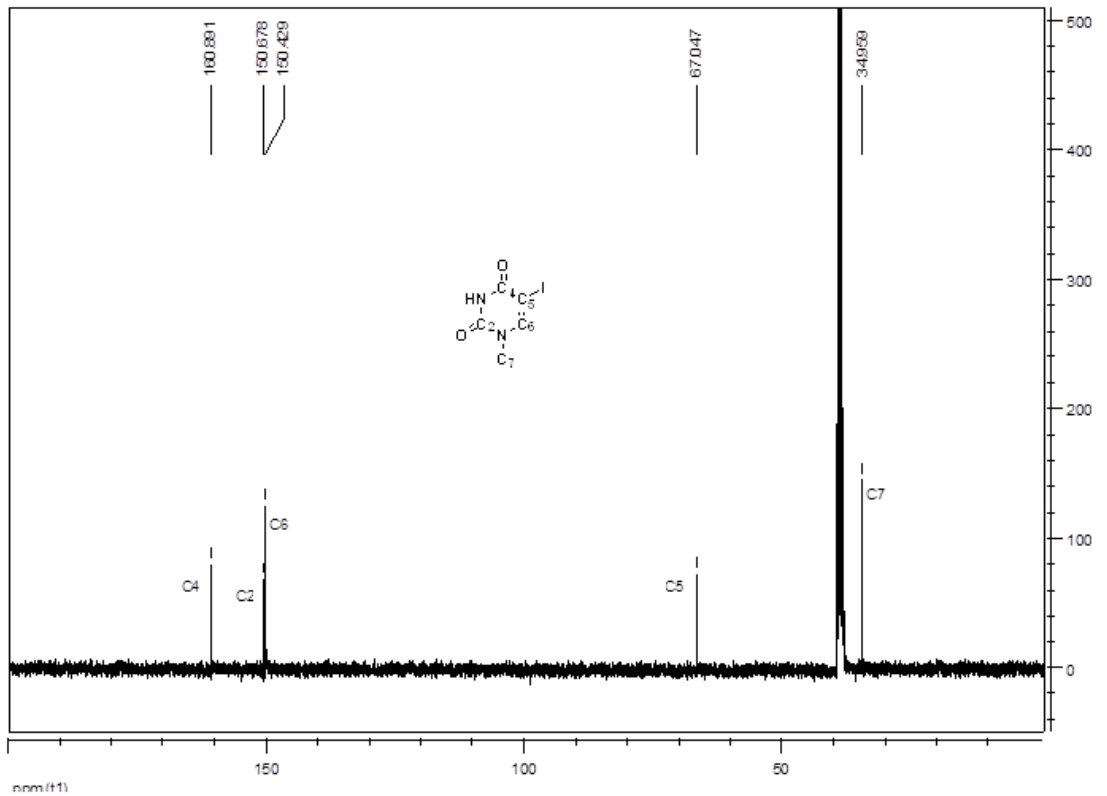

[13]CNMR of compound **15.**

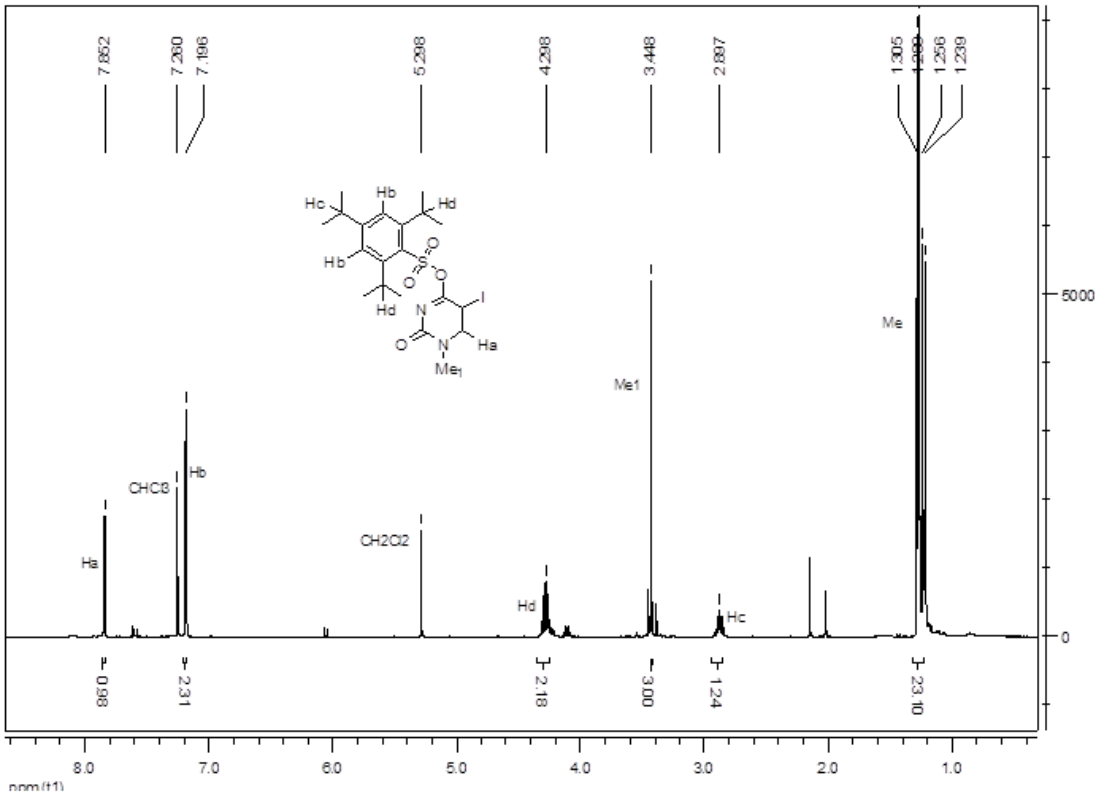

[1]HNMR of compound **17.**

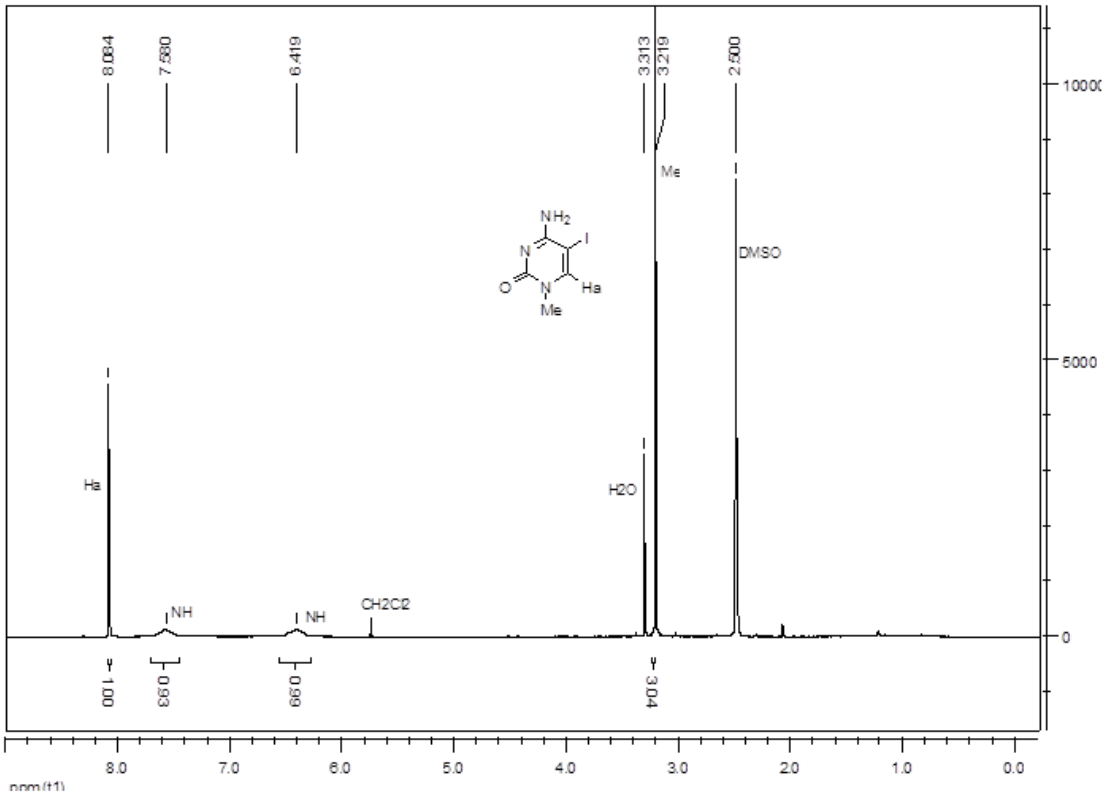

[1]HNMR of compound **18.**

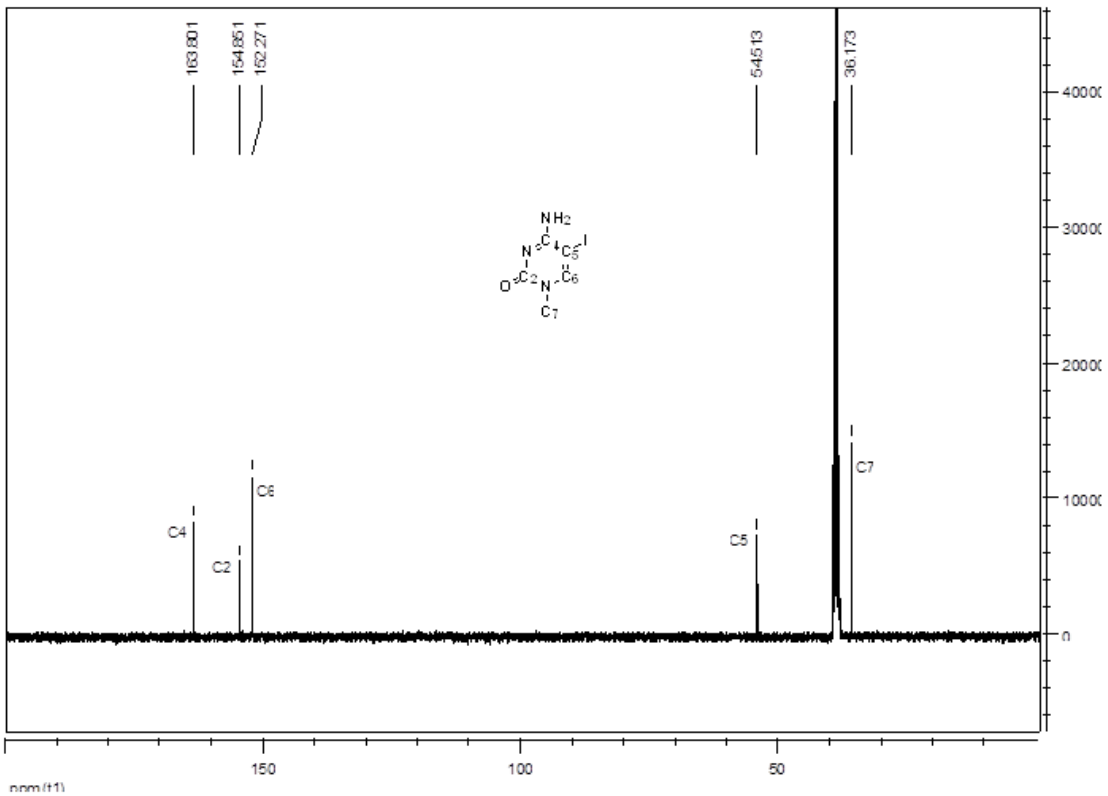

[13]CNMR of compound **18.**

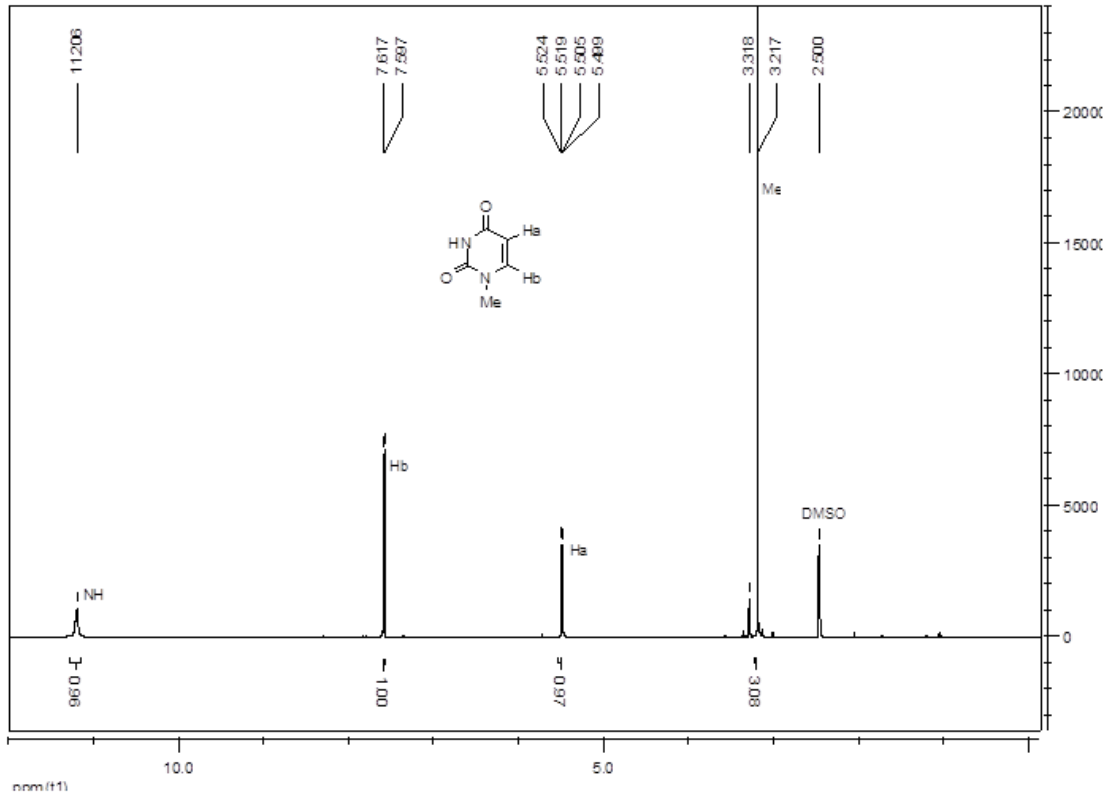

[1]HNMR of compound **19.**

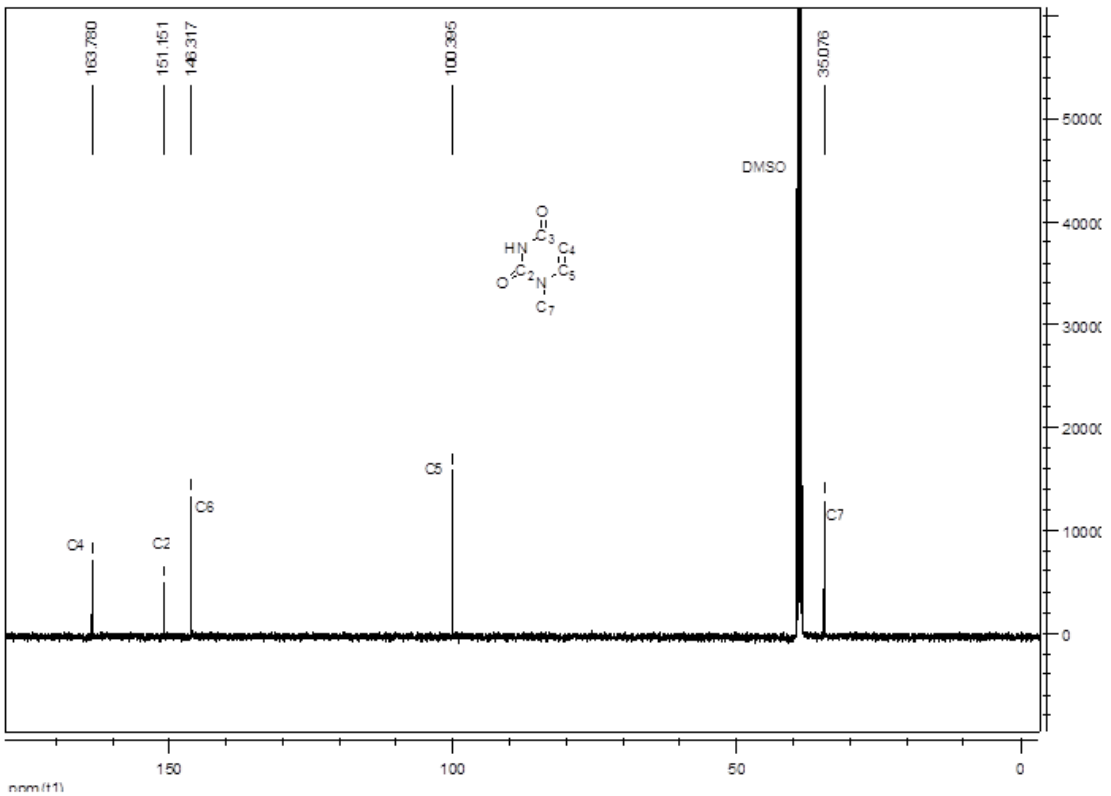

[13]CNMR of compound **19.**

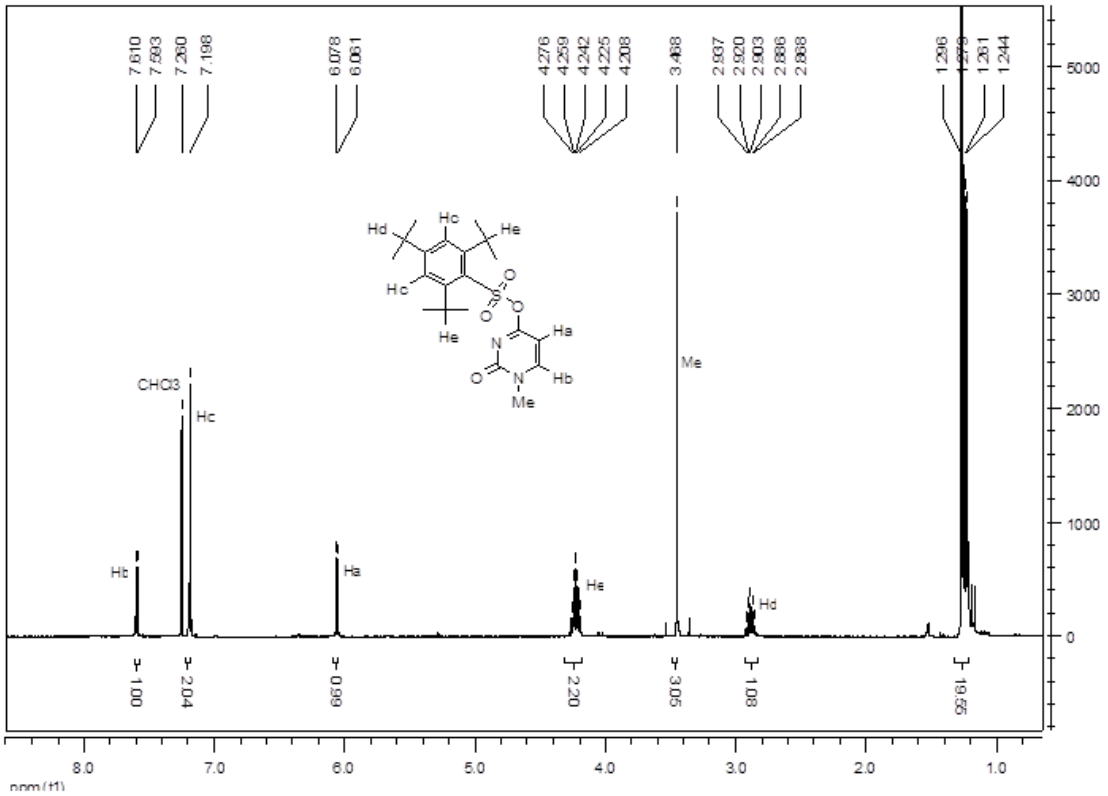

[1]HNMR of compound **20.**

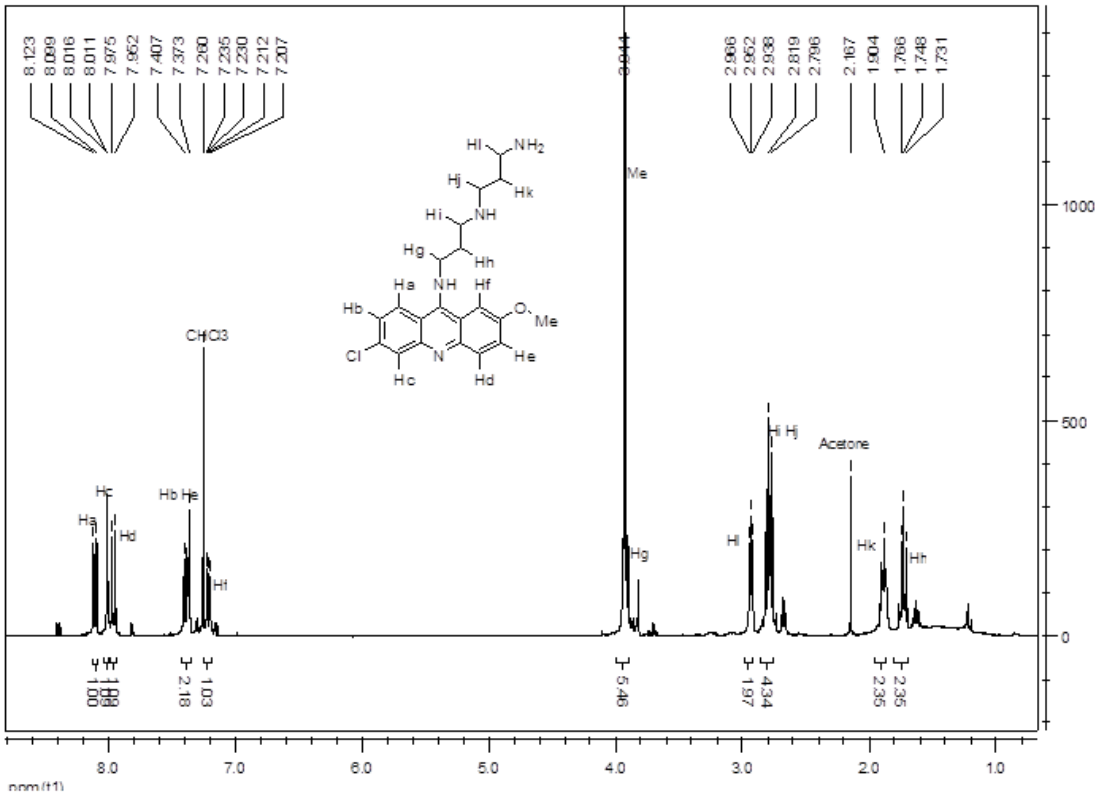

[1]**HNMR** of compound **25**.

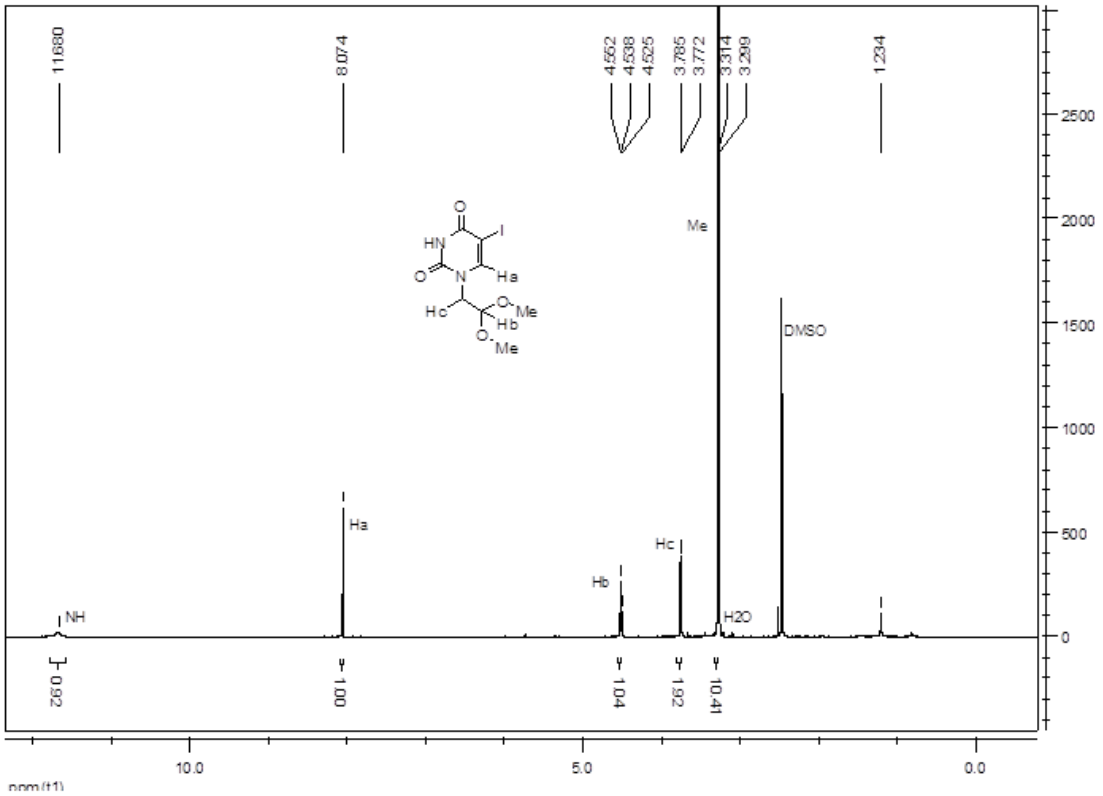

[1]**HNMR** of compound **34**.

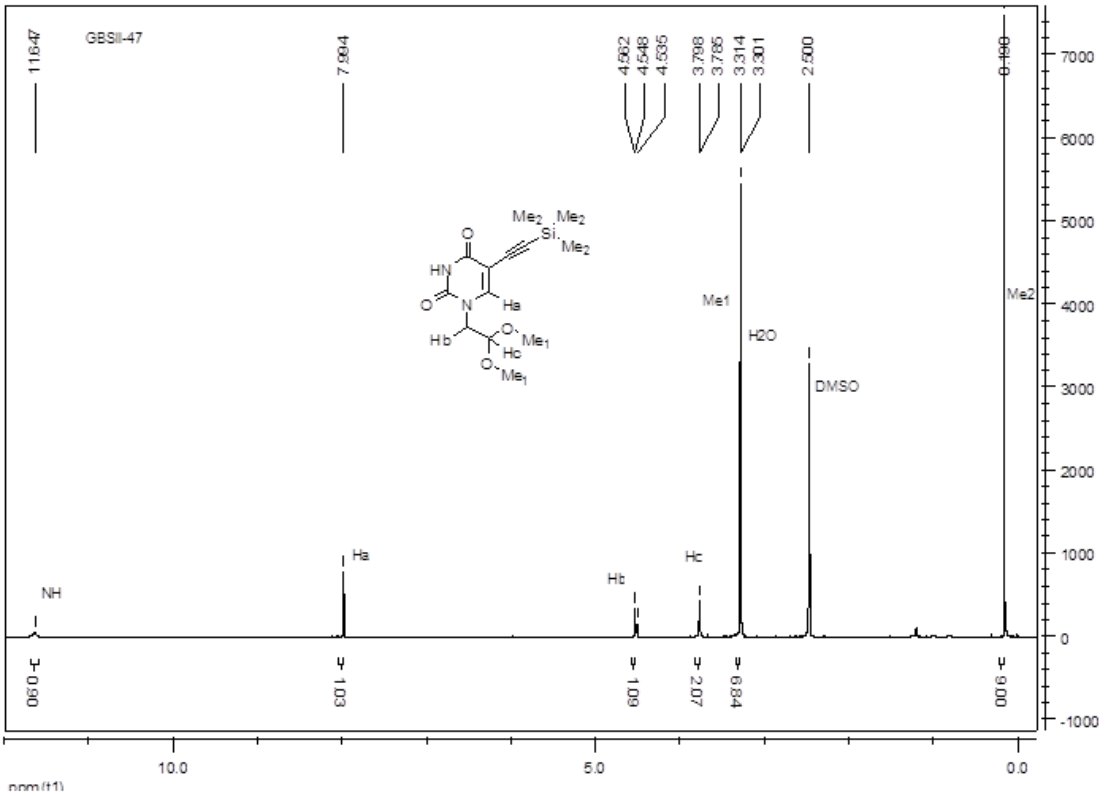

[1]**HNMR** of compound **35**.

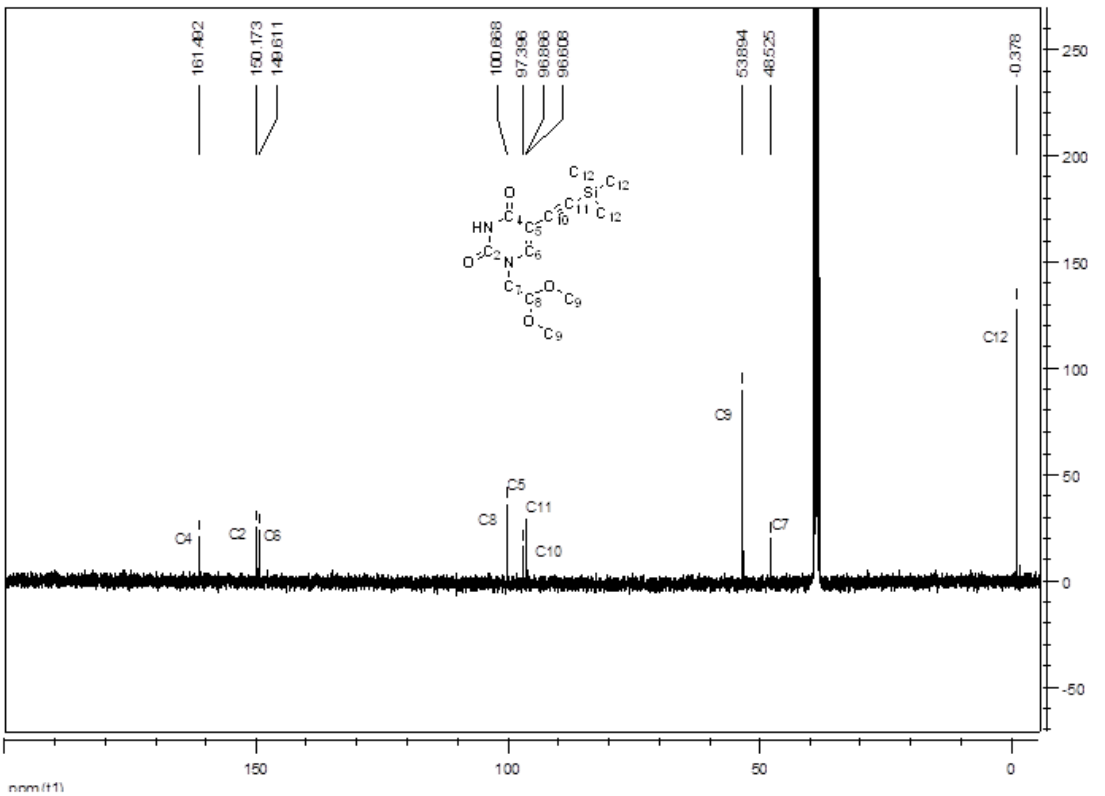

[13]**CNMR** of compound **35**.

5 References

1. He L and Hannon GJ, Micrornas: Small RNAs with a big role in gene regulation, *Nat. Rev. Genet*, 2004. **5**: p. 522-531.
2. Wimberly BT, Broedesen DE, Clemons WM, Morgan-Warren RJ, Carter AP, Vonrhein C, Hartsch T, Ramakrishnan V, Structure of the 30S ribosomal subunit, *Nature*, 2000. **407**: p. 327-339.
3. Bourgeois D, Katona, G, de Rosny, E, Carpentier P, Raman-assisted X-ray crystallography for the analysis of biomolecules, *Methods Mo.l Biol.*, 2009. **544**: p. 253-267.
4. Scott LG, Hennig M, RNA structure determination by NMR, *Methods Mol. Biol.*, 2008. **452**: p. 29-61.
5. Campagne S, Gervais V, Milon A, Nuclear magnetic resonance analysis of protein-DNA interactions, *J. R. Soc. Interface*, 2011. **8**: p. 1065-1078.
6. Kugel, JF, Using FRET to measure the angle at which a protein bends DNA - TBP binding a TATA box as a model system, *Biochemistry and Molecular Biology Education,* 2008. **36:** p. 341-346.
7. Prisner T, Roher M, MacMillan F, Pulsed EPR spectroscopy: Biological applications, *Annu Rev Phys. Chem.,* 2001. **52**: p. 279-313.
8. Schiemann O, Prisner TF, Long-range distance determinations in biomacromolecules by EPR spectroscopy, *Q. Rev. Biophys.,* 2007. **40**: p. 1-53.
9. Sowa GZ, Qin PZ, Site-directed spin labeling studies on nucleic acid structure and dynamics, *In Prog Nucleic Acid Res. Mol. Biol.,* 2008. **82** p. 147-197.
10. Shelke SA, Sigurdsson ST, Site-Directed Nitroxide Spin-Labeling of Biopolymers, *in Unpublished book chapter.* 2011.
11. Kim NK, MuraliA, DeRose VJ, A distance ruler for RNA using EPR and site-directed spin labeling, *Chem. Biol.*, 2004. **11**: p. 939-948.
12. Schiemann O, Reginsson G, Studying bimolecular complexes with pulsed electron-electron double resonance spectroscopy, *Biochem. Soc. T.,* 2011. **39**: p. 128-139.
13. Jeschke G, Polyhach Y, Distance measurements on spin-labelled biomacromolecules by pulsed electron paramagnetic resonance, *Phys. Chem. Chem. Phys.,* 2007. **9**: p. 1895-1910.
14. Smirnova TI, Voinov MA, Smirnov AI, Spin probes and spin labels, *Encyclop. Analyt. Chem.,* 2009.
15. Spaltenstein A, Robinson BH, Hopkins PB, A rigid and nonperturbing probe for duplex DNA motion, *J. Am. Chem. Soc.,* 1988. **110**: p. 1299-1301.
16. Edwards TE, Sigurdsson ST, Site-specific incorporation of nitroxide spin-labels into 2´-positions of nucleic acids, *Nature Protocols,* 2007. **2**: p. 1954-1962.
17. Cai Q, Kusnetzow AK, Hubbell WL, Haworth IS, Gacho GPC, Ned Van Eps, Hideg K, Chambers EJ, Qin PZ, Site-directed spin labeling measurements of nanometer distances in nucleic acids using a sequence-independent nitroxide probe, *Nucl. Acids Res.,* 2006. **34**: p. 4722-4730.
18. Zhang X, Cekan P, Sigurdsson ST, Qin PZ, Studying RNA using site-directed spin-labeling and continuous-wave electron paramagnetic resonance spectroscopy, *Methods Enzymology,* 2009. **469**: p. 303-328.
19. Sigurdsson ST, Nitroxides and nucleic acids: Chemistry and electron paramagnetic resonance (EPR) spectroscopy, *Pure Appl. Chem.,* 2011. **83**: p. 677-686.
20. Shelke SA, Sigurdsson, ST, Noncovalent and Site-Directed Spin Labeling of Nucleic Acids, *Angew. Chem. Int. Ed.,* 2010. **49**: p. 7984-7986.
21. Lindahl T, Karran P, Wood RD, DNA excision repair pathways, *Curr. Opin. Genet. Dev.,* 1997. **7**: p. 158-169.
22. Shelke SA, Noncovalent and site-directed spin labeling of abasic site in duplex DNA with the spin label ç, in *Department of chemistry*. 2011, University of Iceland: Reykjavík. p. 311.

23. Jakobsen U, Shelke, SA, Vogel S, Sigurdsson ST, Site-Directed Spin-Labeling of Nucleic Acids by Click Chemistry: Detection of Abasic Sites in Duplex DNA by EPR Spectroscopy, *J. Am. Chem. Soc.,* 2010. **132**: p. 10424-10428.
24. Jeschke G, Bender A, Paulsen H, Zimmermann H, Godt A, Sensitivity enhancement in pulse EPR distance measurements, *J. Magn. Reson.,* 2004. **169**: p. 1-12.
25. Godt A, Schulte M, Zimmermann H, Jeschke G, How Flexible Are Poly(para-phenyleneethynylene)s? *Angew. Chem. Int. Ed,* 2006. **45**: p. 7560-7564.
26. Shelke AS, Sigurdsson ST, Structural changes of an abasic site in duplex DNA affect noncovalent binding of the spin label ç, *Nucl. Acids Res.,* 2012. **40**: p. 1-9.
27. Fkyerat A, Demeunynck, M, Constant, JF, Michon P, Lhomme J, A New Class of Artificial Nucleases That Recognize and Cleave Apurinic Sites in DNA with Great Selectivity and Efficiency, *J. Am. Chem. Soc.,* 1993. **115**: p. 9952-9959.
28. Gannett PM, Darian E, Powell JH, Johnson EM, A short procedure for synthesis of 4-ethynyl-2,2,6,6-tetramethyl-3,4-dehydro-piperidine-1-oxyl nitroxide*, Synthetic communications,* 2001. **31**(14): p. 2137-2141.
29. Lhomme J, Constant JF, Demeunynck M, Abasic DNA structure, reactivity, and recognition, *Biopolymers,* 1999. **52** p. 65-83.
30. Jereb M, Zupan M, Stavber S, Effective and selective iodofunctionalisation of organic molecules in water and iodine-hydrogen peroxide tandem, *Chem. commun.,* 2004: p. 2614-2615.